KAERI-/TR-767/96

KR9600291

칼리머 원자로구조에 대한
예비 개념설계 및 해석
(Preliminary Conceptual Design and Analysis on KALIMER Reactor Structures)

한 국 원 자 력 연 구 소

제 출 문

한국원자력연구소소장 귀하

본 보고서를 "칼리머 원자로구조에 대한 예비 개념설계 및 해석"에 대한 기술보고서로 제출합니다.

1996년 10월 7일

연구 기관명 : 한국원자력연구소
참여 연구원 : 김 종 범 (액금로설계기술개발)
책임감수위원 : 김 동 훈
감 수 위 원 : 유 봉

요 약 문

본 연구의 목적은 칼리머(KALIMER, Korea Advanced Liquid MEtal Reactor) 원자로 구조물에 대한 예비 개념설계와 예비해석을 수행하여 현재의 예비 개념 연구단계에서의 설계타당성을 분석하고 예측 가능한 문제점을 도출하는 데 있다.

칼리머 원자로 구조물은 원자로용기, 격납용기, 및 원자로 뚜껑으로써 일차 압력경계를 이루고 있으며, 원자로 내부 구조물은 노심의 지지와 구속을 해주는 노심 지지구조물과 노심 제어계통을 지지해주는 노내 상부구조물, 및 고온과 저온의 소디움 풀을 격리하는 역할을 해주고 있는 원자로용기 라이너, 격리판, 열 배플, 및 지지배럴로 구성되어 있다.

원자로구조물의 구조건전성을 보이기 위해서는 계통 열유동해석이 선행되어야 하지만 현재 칼리머에 대한 계통해석 자료가 없기 때문에 본 연구에서는 주요 부품의 열 하중에 대한 제한적인 예비해석을 수행하였다. 해석에 사용된 열 하중은 노심을 통과하는 소디움의 온도 상승, 고온과 저온 소디움 풀의 온도차, 및 각각의 핵연료집합체를 통과하는 소디움의 온도차 등이다.

원자로 용기 및 원자로 내부구조물에 대한 열전달과 열응력 해석은 노심 입출구의 설계온도와 공학적 판단에 기초한 가정치를 사용하였으며 해석에는 상용 유한요소해석 코드인 ANSYS가 이용되었다.

해석 결과 원자로용기, 격납용기, 원자로 뚜껑, 열 배플, 및 격리판에 대해서는 ASME 코드의 설계제한치를 잘 만족하였고 원자로용기 라이너와 지지배럴에 대해서는 설계 타당성과 구조 건전성을 입증하기 위하여 향후 지지배럴의 내벽에 설치할 피막을 고려한 상세한 해석과 부분적인 비탄성해석의 필요성이 대두되었다. 그리고 노심으로부터 올라오는 소디움의 스트라이핑 영향을 줄이기 위하여 노내 상부구조물 하부판에 인코넬 718 라이너의 도입을 제안하였고 또한 열충격 하중을 완화하기 위하여 추가적으로 스테인레스강으로 만든 라이너의 도입을 제안하였으며 단순 예비해석을 통하여 이에 대한 타당성을 입증하였다. 향후 좀 더 자세한 설계자료와 스트라이핑 하중을 보다 정확하게 산출해 낼 수 있는 실험자료 및 열유동 해석자료를 사용한 상세해석이 요구된다.

Summary

The objectives of this study are to perform preliminary conceptual design and structural analyses for KALIMER(Korea Advanced Liquid Metal Reactor) reactor structures to assess the design feasibility and to identify detailed analysis requirements.

The principal reactor structures are the reactor vessel, containment vessel and closure head which form the primary pressure boundary, support barrel and core support structure which provide core support and core restraint, the reactor vessel liner, separation plate and thermal baffle which, in conjunction with the support barrel separate the hot and cold pools, and the upper internal structures which support the core control system structures. The structures separately or together also support thermal insulation and shielding and define the coolant flow paths and shutdown heat removal paths.

Demonstration of design feasibility for the reactor structures requires system thermal-hydraulic, structural, and neutronic analyses. Component responses to these system loads would be compared with design limits to assess the design adequacy. However, KALIMER thermal hydraulic system analysis results and neutronic analysis results are not available at present, only limited preliminary structural analyses have been performed with the assumptions on the thermal loads.

The main sources of thermal loads in the reactor system are a) the sodium temperature rise through the core, b) the temperature differences between the hot pool sodium and the reactor structure support, and c) the temperature differences in sodium exiting from the various core assemblies. The preliminary thermal and structural analyses were limited to the structures affected by these loads.

The responses of reactor vessel and reactor internal structures were based on the temperature difference of core inlet and outlet and on engineering judgments. Thermal stresses from the assumed temperatures were calculated using ANSYS code through parametric finite element heat transfer and elastic stress analyses. While, based on the results of preliminary conceptual design and structural analyses, the ASME Code limits for the reactor structures were satisfied for the pressure boundary, the needs for inelastic analyses were indicated for evaluation of design adequacy of the support barrel and the thermal liner. Such analyses would require detailed thermal-hydraulic analyses results to define the system loads as well as high temperature material data base necessary for the analyses.

To reduce thermal striping effects in the bottom area of UIS due to up-flowing sodium from reactor core, installation of Inconel-718 liner to the bottom area was proposed, and to mitigate thermal shock loads, additional stainless steel liner was also suggested. The design feasibilities of these were validated through simplified preliminary analyses. In conceptual design phase, the implementation of these results will be made for the design of the reactor structures and the reactor internal structures in conjunction with the thermal hydraulic, neutronic, and seismic analyses results.

Table of Contents

List of Tables

List of Figures

1. Introduction

The KALIMER[1] structural design approach is similar to the LWR design approach but requires consideration of the following principal differences in the structural design requirements.

1) The KALIMER operates at considerably higher temperatures which introduce material damage from creep and creep-fatigue interactions and the associated creep-rupture, ratchetting and creep-buckling failure modes. This requires nonlinear time-dependent analyses to assess the structural response to the duty cycle loads and the use of the elevated temperature code cases of the ASME Code to verify structural integrity. This in turn requires development of appropriate analysis methods and material properties not available in the Code.

2) The 146 °C temperature rise through the KALIMER core far exceeds the temperature rise in the LWR cores with a corresponding increase in temperature gradients, thermal stresses and thermal fatigue cycles requiring use of flexible structures and complicating creep-fatigue evaluations.

3) The sodium coolant in the KALIMER. while eliminating the water chemistry problems, affects the material properties by erosion, corrosion and interstitial transfer. The ASME Code data base has to be supplemented to account for these effects.

4) The need to preclude sodium leaks requires the control rods to be inserted and manipulated from the top of the reactor. The necessity to protect and guide the control rod drivelines from the drive mechanisms above the reactor closure into the control assembly ducts in the core dictates the presence of a stiff structure just above the core. The temperatures differences in the coolant streams impinging on this upper internal structure produce high cycle thermal striping loads which far exceed the ASME Code data base for fatigue limits.

5) In most LMR designs including the KALIMER, the core is supported from the reactor vessel bottom head and the control rods are supported from the reactor closure. Also, the structural material in the core is minimized to maintain fast neutron spectrum which requires the core to be made of free-standing assemblies packed together and supported only on the periphery. The functional failure modes arising from these geometrical arrangements are unique to the LMR designs.

6) The KALIMER operates at near-atmospheric pressures. Therefore structural loads during normal operation are insignificant. However, the design is still constrained by the opposing requirements for strong structures to withstand seismic loads and flexible structures to accommodate large thermal loads.

The objectives of this study are to perform preliminary conceptual design and structural analyses for KALIMER reactor structures to assess the design feasibility and to identify detailed analysis requirements. Demonstration of the reactor structures design capability requires system thermal/hydraulic, structural, and neutronic analyses. Component responses to these system loads would be compared with design limits to assess the design adequacy. Since KALIMER system analysis results are not available at present, only limited preliminary analyses have been performed focused on the thermal loads. In the absence of system thermal-hydraulic analyses, the component responses to the above thermal loads were based on core inlet and outlet design temperatures with temperature distributions based on engineering judgment.

2. Preliminary Design of KALIMER Reactor Structures

KALIMER is a pool-type liquid metal reactor. The reactor structures, shown in Figure 1, consist of the containment vessel, reactor vessel, reactor closure,

intermediate heat exchangers (IHX), electromagnetic (EM) pumps, control rod drives, reactor internal structures, and the structure support structure.

The reactor vessel and containment vessel are attached to the reactor closure and are the major components of the reactor enclosure which provides the container and support structure for the reactor core, primary sodium, and structures within. The reactor vessel performs its support and container functions during all temperature, pressure, and load variations which occur during the operating lifetime. The reactor vessel has no penetration and no attachments other than those for connecting the core support structure to the hemiellipsoidal (TBD) bottom head and those used as temporary shipping supports. The reactor vessel is suspended from the closure. The closure is supported on the containment vessel flange, which in turn is supported from the structure support structure. The dimensions of the reactor and containment vessel are sized not only to hold the core and perform as a reactor system but also to have sufficient surface area to transfer decay heat by direct convection and by radiation to the collector cylinder for removal by natural circulation of air.

The principal function of the reactor internal structures is to provide the mechanical support and restraint of the reactor core. These structures also participate in providing restraint for the primary components, providing control and direction of the primary coolant within the reactor system, and supporting the in-vessel shielding necessary for biological protection. Those components that comprise the reactor internal structures are schematically shown on Figure 1. Except in the few cases indicated below, all the internal structures are fabricated from austenitic stainless steel, thus eliminating concerns over oxidation, differential thermal expansion, dissimilar metal

welds and post-weld heat treatment.

2.1 Reactor Vessel

The reactor vessel (shown in Figure 1) is the immediate support and container for the primary sodium and the reactor internal structures. The core support structure makes direct welded connection near the bottom head of the vessel. Other than the core support connections and any shipping restraints, the vessel has no attachments and no penetrations. The weight loads of the reactor internal structures are transferred to the reactor vessel through the core support attachment. The vessel carries those loads and the weight of contained sodium in tension up to its integral connection with the reactor closure.

A cylindrical shell with integral hemiellipsoidal shell (the bottom head) makes up the reactor vessel. The overall dimensions of the reactor vessel were established with consideration of the requirements for sodium level, RVACS surface area, and refueling operations. The need for maintaining the sodium level above the IHX inlet including potential vessel leak determined the reactor vessel's diameter. Significant dimensions and some relevant design data are given in Table 1.

Construction of the reactor vessel shall meet the requirements of Section III and Code Cases N-47[2] through N-51 of the ASME B&PV Code for Class 1 components. Service conditions of the reactor vessel are TBD. Under abnormal conditions the reactor vessel is subjected to temperatures higher than 427 °C and ASME Code Case N-47 is therefore applicable for design. During normal operation, however, the 533 °C reactor outlet sodium wets only the vessel liner; whereas the sodium wetting the vessel is at a level 300 cm lower and a temperature about 146 °C lower (TBD). The drawn-down level between

the vessel liner and the reactor vessel reduces temperature differences along the length of the vessel and greatly lessens concerns about creep damage and deformations in the vessel wall.

Service condition pressures are (TBD). These are based on the sodium/cover gas volume and temperature changes in the reactor vessel and in the annulus between the reactor vessel and containment vessel.

2.2 Containment Vessel

Several functions influence the design of the containment vessel. The containment vessel is classed as a nuclear component governed by the requirements of Section III of the ASME B&PVC. Possible service as a container for leakage of sodium from the reactor vessel means that the containment vessel could be subjected to temperature higher than 427 °C, which is not permitted by ASME Code Class MC. Therefore the containment vessel is designed to meet the rules of Subsection NB of Section III and the high temperature Code Cases N-47 through N-50. For its radiant heat transfer function in the RVACS, its construction will include special measures to provide surfaces with emissivities that meet design requirements. Lastly, the containment vessel flange is part of the support structure for the reactor structure. The load of the reactor structure is transferred through the flange to the reactor structure support subsystem. The compression load on the containment vessel flange is beneficial to maintenance of the seal between flange and closure.

Dimensions and other design data for the containment vessel are listed in Table 2. The containment vessel length is slightly greater than that of the reactor vessel, and like the reactor vessel, provides the required RVACS heat

transfer surface area. The length and diameter also limit the volume between the containment vessel and reactor vessel. With the limited volume, sodium leakage from the reactor vessel will not lower the sodium level sufficiently to prevent continuance of flow into the IHX's and retention of the core cooling circuit.

The cylindrical shell of the containment vessel terminates at the top in a deep flange. The flange is bolted and sealed to the reactor closure. The seal between the containment vessel and reactor vessel is an Omega seal which is welded to the containment vessel flange and the reactor closure. The bottom head of the containment vessel is hemiellipsoidal with contour like the head of the reactor vessel. The containment vessel normally operates at temperatures which are TBD.

2.3 Closure Head

The closure head is the top head of both the reactor vessel and the containment vessel, and is a major element of the containment boundary. It is designed to operate at comparatively low temperatures (90 °C~150 °C) - (TBD). The low operating temperature is attained by inclusion in the design of horizontal layers of stainless steel plates, which are TBD, under the closure head and supported from the closure head.

The main structural plate of the closure is 50 cm thick and 1150 cm in diameter. At its outer edge it rests on, and is fastened and sealed to, the wide top flange of the containment vessel. The equipment for which the penetrations are made are, in general, supported by the closure. The closure is designed for the normal and seismic loads applied to it by its own weight, the applied equipment loads, and attached shield/insulation weights, in

combination with the cover gas pressures and service conditions. The design requirements include a deflection limit (TBD) based on seismic reactivity analyses.

A thin layer of thermal insulation covers the top surface of the closure. All structural parts of the closure, other than bolting, are constructed of Type 304 stainless steel. The choice of bolting materials depends on function and environment, but is, in general, high alloy steel. The material for non-structural parts depends on function and environment.

The functions of the closure require that it be considered a Class 1 nuclear component governed by the requirements of Section III of the ASME B&PVC. The application of Code Case N-47 or the related code cases for elevated temperature construction is not necessary, however, so design and construction will be in accordance with Subsection NB.

2.4 Reactor Structure Support

The reactor structure is supported by twelve radial support arms welded to the containment vessel flange. The support arms rest on Lubrite plates which are anchored to a circular recessed steel ledge embedded in the Head Access Area (HAA) floor adjacent to the reactor structure. The Lubrite plates permit radial thermal displacements while providing vertical support. Lateral seismic restraint is provided by the close fit of the support arm bolts within the radially slotted holes in the arms.

The radially slotted holes allow the support arms to move radially, relative to the stationary anchor bolts, as the top end of the reactor structure cycles through its temperature range. The attachment is designed to resist structure

motions and accelerations relative to the support ledge occurring during seismic events.

2.5 Core Support Structures

The core support structure provides the restraint of the reactor core assemblies necessary to maintain them in their prescribed geometry during all modes of reactor operation. This integrally welded structure is attached to the reactor vessel shell and bottom head, also by welding, to form a rigid radial beam structure. This approach has large design margins and the added advantage that the consequences of failure in a given member is negligible. The core support is located in the bottom end of the reactor vessel where the operating temperature is the lowest of the entire system and thermal transients, because of the distance from their sources, will be negligible.

The core support function is subdivided into lateral and vertical restraint. Each sub-function is provided in a different fashion by the core support structures. For lateral restraint, the core assemblies are held (1) by their nosepieces in the receptacles, and (2) by the load pads near the top of the assemblies which are surrounded by a core former ring attached to the support barrel. The separation of the assemblies is maintained by an intermediate plane of load pads at an elevation above the active core. Positioning of the handling sockets is also maintained by the top load pads. The intermediate load pads above the core are not restrained by former rings attached to the support barrel. Thus, the core assemblies are free to bow as dictated by temperature differences and their metallurgical condition. Load transfer is through the core assembly load pads to the plate segments and then to the former ring and the support barrel.

The inlet plenum, located in the central region of the core support structure and below the core, receives primary sodium from four pipes and distributes it to the core via the nosepiece receptacles. There are 391 receptacles (one for each core assembly). These are located in a triangular pitch to match the core array map. The receptacles participate in the core orificing. The depth of the inlet plenum is established by the space required for the inlet piping nozzle forging welds and the radial flow area necessary to assure uniform flow distribution to all the core assemblies. This flow distribution is further enhanced by the design of the receptacles which are necked down on their lower end to increase the available flow area.

Structurally, the inlet plenum is comprised of two horizontal flat plates, a large diameter cylinder, and six (TBD) small diameter tie rods. These components form a can-like volume. The upper plate is connected to the lower plate through the six (TBD) tie rods and the perimeter cylinder that carry the pressure loads tending to separate the plates. All of the vertical loads from the core assemblies are carried, through the receptacles to the lower grid plate. The upper grid plate serves to accurately position the receptacles and also participates in sealing the annulus around each of the receptacles and transmittal of lateral seismic loads to the support barrel. The lower plate is supported from the vessel by eight radial plate beams.

2.6 Support Barrel

The support barrel is the structural member extending vertically upward from its attachment at the core support structure to the upper regions of the reactor hot plenum. It has a 400 cm outside diameter and is 5.0 cm thick. The function of the support barrel is to provide a base of support for all the reactor

internal components. It also serves as the boundary between the reactor hot plenum and cold plenum regions and thus provides both thermal insulation and low pressure separation between these regions. Lower part of the support barrel provides lateral support to the core. The core lateral loads are transmitted to the support barrel through the upper grid plate at the core inlet plenum and through the core former ring at the top load pad elevation. The support barrel also provides:

1) Lateral support of the near core fixed radiation shielding; (TBD)

2) Lateral and vertical support of the separation plate and reactor vessel thermal liner; lateral support of the EM Pump's and IHX's through the separation plate;

3) Support of the B_4C IHX shielding; (TBD)

4) Support of the horizontal baffle.

Structural interfaces associated with each of the above functions are discussed below with the specific components.

2.7 Reactor Vessel Liner and Separation Plate

The reactor vessel liner provides steady state and transient thermal protection for the vessel and forms a portion of the pressure boundary between the hot plenum and the cold plenum regions within the reactor. This boundary is completed by the separation plate which spans the gap between the liner and the support barrel. The thermal liner provides support for the horizontal baffle which forces thermal stratification in the upper volumes of the cold pool and thus minimizes heat transfer between the hot and cold pools.

The vessel liner is a cylindrical member located 7 cm inside the reactor vessel. It is provided with slots at its top end that under normal operating conditions are always above the sodium level. During reactor operation these slots are approximately 30 cm (TBD) above the hot pool sodium level and the cold pool communicates freely with the annulus between the liner and the reactor vessel at the support plate elevation. The free surface of the sodium within the inner annulus formed by the vessel and the liner will be approximately 300 cm (TBD) below the hot pool free surface due to the IHX primary pressure drop. This causes the portions of the reactor vessel adjacent to the hot pool to be exposed to cover gas over their entire length thus helping to insulate the vessel and minimize steady state heat losses to the RVACS. The liner also isolates the reactor vessel from rapid temperature changes in the hot pool sodium that result from duty cycle events. thus minimizing the thermal loading on the vessel, its attachment to the reactor closure, and to the containment vessel.

The bottom end of the liner is welded to horizontal separation plate. The separation plate has a number of circular penetrations that allow the IHX's and the primary pumps to pass through while providing a lateral seismic support for these components.

During events requiring RVACS for total heat removal, the reactor resident sodium heats up, expands, and flows through the liner slots. Since the pumps are not operating in this event, the sodium level is the same on both sides of the liner. A significant fraction of the hot pool sodium bypasses the inoperative IHX's and is cooled through the reactor vessel wall. The cooled sodium sinks to the bottom of the vessel where it is drawn into the pump intake and directed back to the core to complete the circuit.

2.8 Hot Pool Thermal Insulation

Insulation is provided between the reactor's hot pool and cold pool to reduce the amount of energy bypassing the IHX's. This insulation, which is comprised of various components, is typically used primarily to satisfy some other function. Basically the insulation is formed by the support barrel and IHX shielding attached to the inside and outside surfaces of the support barrel and by the horizontal baffle. (TBD)

2.9 Upper Internals Structure

The upper internals structure (UIS) will be attached to the UIS plug of the reactor closure and cantilevered downward into the reactor hot pool. Its bottom end of shroud tube will be located 5.0 cm (TBD) above the top of the core assemblies during power operation. The principal structural functions satisfied by the UIS are: (1) lateral support of the control rod drivelines, (2) protection of the drivelines from sodium flow induced vibration, (3) support of the above core instrumentation drywells, and (4) sodium mixing and isolation of downstream components from core exit thermal environment.

The UIS is plugged in during power operation and plugged out while refueling. Design details are to be determined.

Shroud Tubes - There is one shroud tube assembly for each of the nine control rod drivelines. Each assembly consists of an upper SS-316 tube, a lower Inconel Alloy 718 tube, and an internal bushing. The tubes are sized and located such that the drivelines pass through the center of the assemblies without contacting the tubes except over a region near mid-elevation where a close fitting guide bushing is located. Inconel Alloy 718 was selected for the

bushing because of its mechanical wear properties. Inconel Alloy 718 was also selected for the lower tube to sustain the thermal striping and thermal shock conditions existing near the core outlet. (TBD)

Instrumentation Drywells - There are twenty drywells routed from the top of the UIS plug to the region directly above the reactor core. These pass through and are supported by the UIS. Details are (TBD).

UIS Structures - The principal structural member of the UIS is the 240 cm diameter SS-316 cylinder that extends down to approximately 90 cm above the core outlet. The cylinder's wall thickness of 2.5 cm was selected to assure adequate resistance to seismically induced displacements thus satisfying requirements on the motions of the control rod drivelines relative to the core. Additional stiffness for the cylinder is obtained from the three horizontal plates that are welded to its walls. The bottom end of the structure is provided with two liners that protect it from the thermal environment at the core outlet. The outermost liner is made from Inconel Alloy 718 and is used for thermal striping protection. The second SS-316 liner, in conjunction with outer liner is used to insulate the structure against rapid temperature changes occurring during scram transients. (Details are TBD)

3. System Analysis

KALIMER structural evaluations follow the same scheme as the LWR evaluations which basically consist of system analyses to calculate the component loads, subsystem and component analyses to calculate the component stresses and deflections, and design margin evaluations based on comparison of the calculated stresses and deflections with the appropriate

stress limits and functional deformation limits.

The KALIMER reactor is to withstand the design basis duty cycle, and, as a goal, various bounding events used to assess the safety design margins, within the limits of the ASME Code. Demonstration of compliance to these limits requires system thermal-hydraulic, structural and neutronic analyses of this entire set of events. Component structural loads would be obtained from system seismic and structural analyses and thermal loads and velocity fields would be obtained from system thermal-hydraulic analyses. KALIMER system thermal hydraulic analysis results are not available at present. This section summarizes the assumptions used in the component analyses in the absence of this information.

3.1 Thermal Hydraulic Analysis

KALIMER system thermal hydraulic analyses, which are under progress, will produce detailed three dimensional flow patterns and temperature distributions for normal operation and thermal transients. This information will be then used in component heat transfer and thermal stress analyses and reactor creep damage evaluations. The velocity fields from the thermal hydraulic analysis will be used for evaluation of flow induced vibrations.

Thermal-hydraulic analysis results for KALIMER are not available at present. Therefore the component heat transfer and thermal stress analyses for the preliminary design concept evaluation are based on the following temperature conditions postulated on the basis of other LMR references.

Steady State Temperature Distribution: KALIMER outlet plenum sodium temperature is 533 °C and inlet plenum sodium temperature is 387 °C. These

temperatures are assumed to apply to the structural surfaces in contact with the hot and cold sodium pools respectively as shown in Figure 2. The closure upper surface is assumed to be at 93 °C. It is assumed that thermal insulation attached to the closure head will be designed to limit the temperature drop across the closure thickness to be less than 10 °C. RVACS air outlet temperature is assumed to be 93 °C uniform for the purpose of current conceptual design evaluations and applied to containment vessel outer wall. These temperatures are used in heat transfer and thermal stress analyses.

Transient Temperature Distribution: Sodium mixing and stratification in the long support barrel in the KALIMER design protect the outlet plenum structures and components from the core exit environment. Therefore the most severe thermal transients will be limited to the structures at the UIS bottom end. These structures were analyzed for scram transients assuming sodium temperature to decrease from 560 °C to 390 °C. Parametric analyses were performed for a range of transient temperature rates and sodium film coefficients to envelop different transients and potential thermal environment which are not defined at present. UIS response to thermal striping loads was evaluated for core exit coolant striping between 433 °C and 633 °C. Parametric analyses were performed for a range of film coefficients and striping frequencies.

3.2 Seismic Analysis

KALIMER system seismic analyses will provide reactor system seismic loads and deflections which will be then used in component stress and deflection analyses. The seismic stresses will be combined with the pressure. gravity and thermal stresses and compared with the appropriate stress limits

and the seismic deflections will be used to determine the margins to functional design limits.

Preliminary reactor system seismic analyses have been performed with finite element code. The analysis models include the seismic isolators which are modeled as a combination of translational and rotational springs with the properties selected to yield the system isolation frequency. Analysis results identify the benefits of seismic isolation on the reactor design as well as simplify the analyses[3].

3.3 Neutronic Analysis

The reactor system design limits include the limits on seismic reactivity insertions resulting from the core and control rod separation under seismic loads. The limits may be based on the requirement of precluding super-prompt criticality from instantaneous reactivity insertion or on the more stringent assumption of absence of scram with a requirement of limiting fuel failures due to cyclic reactivity insertions. Core neutronic analyses would provide the seismic reactivity insertions which would produce these conditions. These reactivity insertion limits will be then translated into seismic deflection limits for the reactor structures.

4. Component Stress Analysis

Pressure and gravity stresses in the KALIMER reactor system would be small because of the near-atmospheric operating pressure and the relatively thick reactor vessel wall. Therefore the reactor system design would be governed by the seismic and thermal loads. The seismic loads have been analyzed and discussed in the reference [3]. Therefore the preliminary

analyses of the KALIMER reactor system design were focused on the thermal loads.

The sources of thermal loads in the reactor system are a) the large temperature rise of 146 °C through the KALIMER core, b) temperature difference between the hot pool sodium and the low temperatures of the reactor structure support system and the head-access area above the reactor closure, and c) the large temperature gradients in the core exit region because of the temperature variations in the different core assembly sodium. The preliminary thermal stress analyses are limited to the reactor structures affected by these loads. Specifically, the 146 °C temperature rise through the core would produce large thermal stresses in the support barrel, separation plate, thermal liner, and baffle plate which serve as a boundary between hot pool sodium and cold pool regions. . The temperature drop from the hot pool sodium to the reactor support system would produce thermal stresses at the reactor/containment vessel and the closure interfaces which would depend on the closure insulation and the reactor system support design. The core assembly sodium temperature differences and variations would produce thermal striping and transient loads at the UIS bottom end which will be exaggerated by the high temperature.

The preliminary thermal stress analyses are based on assumed thermal hydraulic conditions because proper thermal hydraulic data for KALIMER is not available yet. The objective of analysis is not to obtain detailed coordinated design evaluation but to find out the point at issue with simplified rapid evaluation method. These are described below and detailed coordinated evaluation with required thermal hydraulic analysis results and design data

will be done in next design stage.

4.1 Reactor Vessel and Containment Vessel

A steady state heat-transfer analysis of the structures in the upper sodium pool region of the KALIMER reactor was performed using the ANSYS finite element computer code[4]. Temperature distributions for the reactor vessel, internal hot pool structures, and containment vessel were calculated and corresponding thermal stresses were evaluated. These stresses were compared to the stress limits of ASME Code and the adequacy of preliminary design of KALIMER reactor vessel and containment vessel was tentatively ascertained. The detailed evaluations are described in the following subsections.

4.1.1 Heat Transfer Analysis

Analysis Model:

Temperature distributions in the containment vessel, reactor vessel, and the box-ring structure consisting of the thermal liner, baffle plate, separation plate, and support barrel were calculated using the ANSYS finite element code. The analysis model is shown in Figure 3. The upper boundaries of the model shown in Figure 3 are the top ends of reactor vessel and containment vessel attached to the closure head (elevation -0.5 m with the closure head top end assumed to be at zero elevation.) The lower boundaries of the model are at elevation -7.95 m for the support barrel, elevation -7.45 m for the reactor vessel and containment vessel, and the bottom of the separation plate.

The ANSYS axisymmetric heat transfer analysis model shown in Figure 3 consists of 1496 nodes, 1290 PLANE75 (four-node axisymmetric harmonic thermal solid) elements and 152 LINK31 (one dimensional radiation link)

elements. ANSYS PLANE75 elements with thermal conduction and convection capabilities were used for modeling the SS316 reactor structures and the 2.25Cr-1Mo containment vessel. The sodium inside the box-ring structure also modeled using PLANE75 elements was assumed stagnant. (Convection in this region was ignored in the analyses since ANSYS does not have fluid flow analysis capability. This is a conservative assumption since convection currents in the ring box are expected to decrease the temperature gradients.) The annular sodium between thermal liner and the reactor vessel modeled using the PLANE75 elements was also assumed to be stagnant. ANSYS LINK31 elements were used to model radiation across the gaps between thermal liner and reactor vessel, reactor vessel and containment vessel, and containment vessel and RVACS airflow.

Loads and Boundary Conditions:

The steady state thermal analysis representing normal operation was performed with following thermal loads and boundary conditions. Inner surface of the support barrel, upper surface of the baffle plate, and inner surface of the thermal liner were assumed to be at the hot pool sodium temperature of 533 °C. The bottom of separation plate and the bottom of the sodium column in the reactor vessel/thermal liner annulus (elevation -7.45 m) were assumed to be at the cold pool sodium temperature of 387 °C. Heat transfer between reactor vessel and thermal liner below the annulus sodium free surface was assumed to be by conduction through the annular sodium neglecting any convection. Heat transfer between the reactor vessel and thermal liner above the annulus sodium free surface as well as between the reactor vessel and containment vessel were assumed to be by radiation neglecting any convection effects. Top and bottom ends of the reactor vessel and containment vessel in the model were assumed to be adiabatic since the

area of concern in this analysis was far from these end boundaries.

RVACS outgoing air was assumed to be at uniform temperature of 93 °C (appropriate boundary conditions for the containment vessel outer surface require thermal hydraulic tests and analyses including RVACS inflow air and collector cylinder walls which are only in the planning stage.) The convection film coefficient and emissivity for the containment vessel outer surface contacting RVACS outflow air were assumed as 11.358 J/sec-m^2-°C and 0.8 respectively. The emissivity between liner and reactor vessel was assumed as 0.2 and the emissivity between reactor vessel and containment vessel was assumed as 0.7.

The natural circulation in the confined sodium within the box structure was neglected and heat transfer in this region was considered only by conduction through sodium. The radiation effect for the structures above hot pool sodium free surface was neglected at this stage due to the lack of information on the thermal insulation design below closure head. The radiation analyses between free surface of hot pool and reactor vessel and thermal liner are necessary to be added to current analysis to produce more accurate results.

The temperature dependent material properties used in this analysis (density, thermal conductivity, specific heat, thermal expansion coefficient, Young's modulus, and Poisson's ratio) are listed in Table 3.

Analysis Results:

Steady state heat transfer analysis was performed and temperature distributions were calculated for the reactor vessel and containment vessel over the region bounded by elevation -0.5 m to -7.45 m. Figure 4 shows

temperature distributions at the inner and outer surfaces of the reactor vessel and containment vessel. Maximum temperature of 389.2 °C for the reactor vessel occurs at the inner surface near the cold pool sodium free surface (elevation -6.1 m). The maximum radial and axial temperature gradients also occur near the annulus sodium free surface as shown in Figure 5. Thus, maximum thermal stresses are expected to occur in the vicinity of annulus sodium free surface because abrupt temperature changes produce large thermal stresses both in the axial and hoop directions. In addition to the region near the annulus sodium free surface, large thermal stresses are expected in the reactor vessel in the region across the hot pool sodium free surface (elevation -3.1 m) which has the second largest temperature gradients.

Temperature distribution profiles in the containment vessel are similar to those for the reactor vessel but the magnitudes of the temperatures and the radial and axial temperature gradients are lower than those in the reactor vessel. Thus smaller thermal stresses are expected to be present in containment vessel.

4.1.2 Thermal Stress Analysis

Steady-State Operation:

Large changes in temperature gradients, which induce large thermal stresses, in reactor vessel and containment vessel occur at the annulus sodium free surface elevation (-6.1 m) and the hot pool sodium free surface elevation (-3.1 m). Thermal stresses in these regions were calculated using the ANSYS PLANE42 two dimensional structural solid elements with axisymmetric option.

The 533 °C reactor hot pool sodium wets only the vessel liner during normal operation and the reactor vessel is insulated from the liner and the hot pool sodium by the cover gas. Therefore the vessel remains close to the 387 °C cold pool sodium which wets the vessel at a level 300 cm lower than the hot pool sodium free surface. The analyses described in the previous section predict a maximum vessel temperature of 389.2 °C which is well below the 427 °C temperature limit for the application of ASME Code Subsection NB for stainless steel structures. Therefore it is adequate to compare the thermal stress results under the steady steady condition with ASME Code Subsection NB limits.

In the vicinity of annulus sodium surface (elevation -6.1 m), reactor vessel inner surface has compressive stresses of 88.2 MPa and 129.7 MPa in the axial and circumferential directions respectively. These thermally induced secondary stresses are less than the ASME Code (Section III-NB) secondary stress limit of $3S_m$ (333 MPa for SS316 at 400 °C) and are acceptable. At elevation -3.1 m, reactor vessel inner surface has compressive stresses of 124.5 MPa and 91.9 MPa in the axial and circumferential directions, respectively, which also satisfy the $3S_m$ limit.

The maximum primary stress in the reactor vessel at elevation -6.1 m from gravity (based on the reactor vessel weight and assumed sodium, core and internal structures weight as shown in Table 4) is small (~ 7 MPa) compared to the thermal stress and consequently does not influence the structural integrity.

There may be significant changes in temperature gradients in reactor vessel at the elevation of the thermal insulation below the closure head. However, these are expected to be small compared to the above results. More precise

analysis will be performed when thermal insulation design is developed and radiation heat transfer is analyzed in the hot pool region to calculate these gradients.

Containment vessel operates at much lower temperature and has less severe thermal gradient changes compared to the reactor vessel. These temperature gradients were calculated to produce correspondingly smaller compressive stresses of 31.2 MPa and 25.4 MPa in the axial and circumferential directions respectively at elevation -6.1 m, and 28.2 MPa and 17.7 MPa in the axial and circumferential directions, respectively, at elevation -3.1 m. These stresses are very small compared to the ASME Code (Section III-NB) secondary stress limit of $3S_m$ (370.2 MPa for 2.25Cr-1Mo at 300 °C).

Thermal Transients:

Scram with trip of the primary pumps causing a rapid rise of the cold pool sodium in the annulus between the reactor vessel and thermal liner would produce a large thermal down-shock to these structures. The information such as pump trip rates and rates of change in pressure drop across the IHXs is not available at present. The transient heat transfer and thermal stress analyses for this transient will be performed when the relevant transient conditions are established through thermal hydraulic analyses.

4.2 Closure Head and Reactor Support Structure

4.2.1 Closure Head Structural Analysis

Closer Loads:

Closure head supports its own weight and the weights of equipments supported from the head (2 IHX's, 4 primary EM pumps, and UIS whose

weights were assumed to be 100 tons, 160 tons, and 30 tons respectively, for the purpose of present analysis). In addition, the closure head supports the reactor vessel and its contents including sodium (with total approximate weight of 1315 ton calculated as shown in Table 4). Cover gas pressure loading has been neglected because only normal operation condition is considered in the present analysis where the cover gas is maintained at close to atmospheric pressure.

Analysis Model:

Structural analysis for closure head was performed using ANSYS with SHELL63 four node elastic shell elements having both bending and membrane capabilities. Figure 6 shows the finite element model of the closure head. The 11.5 m closure head was modeled with 0.5 m shell thickness except for the region outside of the reactor vessel which was assumed to have half the thickness of the main plate in order to represent the reduced thickness where the closure mates with the containment vessel flange. Only 180° of the closure head was modeled on account of the symmetry which was enforced by the symmetry conditions ($U_y = \phi_x = \phi_z = 0$) along the x-axis. The perimeter boundaries were assumed to have constraints of zero movement in the vertical direction and zero rotations in both radial and axial directions ($U_z = \phi_r = \phi_z = 0$) as shown in Figure 7. The above boundary condition is believed to be conservative and close to real situation. However, the actual boundary conditions representing coupling between the closure head and the containment vessel flange may be different from above conditions since the closure head rests on and is bolted and sealed to the wide top flange of the containment vessel as shown in Figure 8. Therefore clamped edge condition ($U_x = U_y = U_z = \phi_r = \phi_\theta = \phi_z = 0$) was also analyzed to envelop the analysis results.

Material properties for SS304 used in the analyses are listed below:

	Density (Kg/m^3)	Poisson's Ratio	Young's Modulus (GPa)	Thermal Conductivity (J/sec-m-°C)	Thermal Expansion Coeff. (m/m/°C)	Specific Heat (J/Kg-°C)
90°C	7999	0.271	190.4	16.09	$16.326x10^{-6}$	503.28
150°C	7973	0.276	187.5	17.02	$17.028x10^{-6}$	519.6

Parametric studies with dead weight of closure head, weights of supporting structures like primary EM pump, IHX, and UIS, and boundary conditions explained above were performed with thicknesses ranging from 30 cm to 60 cm in order to obtain optimal thickness of closure head. Analysis results are summarized below:

Thick. (cm)	Case 1 (Simple Supported Boundary Condition)		Case 2 (Clamped Boundary Condition)	
	Max. Displ. (cm)	Max. Stress (MPa)	Max. Displ. (cm)	Max. Stress (MPa)
30	2.07	91.3	0.49	76.8
40	0.946	55.6	0.227	46.6
50	0.521	38.3	0.127	32.0
60	0.323	28.5	0.08	23.7

The maximum deflection occurs near intersection of UIS mounting flange and the IHX center line as shown in Figure 9. The maximum stress intensity

occurs at the same location as the maximum deflection as shown in Figure 10. The stress behavior is mainly bending stresses and these elastically calculated stress intensities for primary membrane stress and bending stress are to be compared to the ASME Code (section III-NB) limit of $1.5S_m$. Since the $1.5S_m$ for SS304 at 150 °C is 206.8 MPa, above results satisfy ASME Code stress limit. However, with consideration of amplification of vertical seismic motion due to the absence of vertical seismic isolator, above results will become larger. With an assumed amplification factor of 3 and considering gravity, results will be four times as large as the above values. Another important factor to be considered in selecting optimum thickness is the deflection limit for closure head which will be determined from functional requirement to satisfy core/closure seismic separation limit. While deflection limit is not available yet, optimum thickness of closure head was selected tentatively as 50 cm only considering stress limit. This will be verified against the core/control rod separation limit at a later time.

Using clamped boundary conditions, maximum deflections decrease significantly and maximum stresses occur near supporting boundaries since any rotation is not allowed at clamped boundaries. However, this boundary condition is extreme case and is not realistic because it does not allow any thermal movement of closure head and end rotation at all. When it is required to reduce the amount of deflection from a design standpoint, making support of containment vessel similar to clamped condition might be a point to be considered. On the other hand, it becomes important to investigate local stress behavior including shear stress of the closure head support region because these areas have relatively large stresses. It is also necessary to study the local effects of flanges, which supports IHX, EM pump, and UIS, on the stiffness of the closure head.

4.2.2 Closure Head Thermal Analysis

Since the closure head temperature and thermal response affects the closure head itself, reactor vessel top, containment vessel top, and reactor support structures, it is desirable to maintain low operating temperature and a small temperature gradient through the closure head thickness so that the thermal stresses and bowing motion of closure head are small. Therefore the closure head will be designed to operate at comparatively low temperatures (90 °C ~ 150 °C) which can be attained by inclusion in the design of horizontal layers of stainless steel plates under the closure head. A thin layer of thermal insulation is assumed to cover the top surface of the closure in order to limit the head access area temperatures

When a plate with thickness t and with free ends is subject to a linear temperature gradient ΔT in the thickness direction, it will bow to have a spherical radius of curvature as shown in the adjoining figure. Its radius R is expressed as

$\frac{t}{\alpha \Delta T}$ and the deflection of center of plate is calculated as:

$$d = \frac{t}{\alpha \Delta T}(1 - \cos\frac{\theta}{2})$$

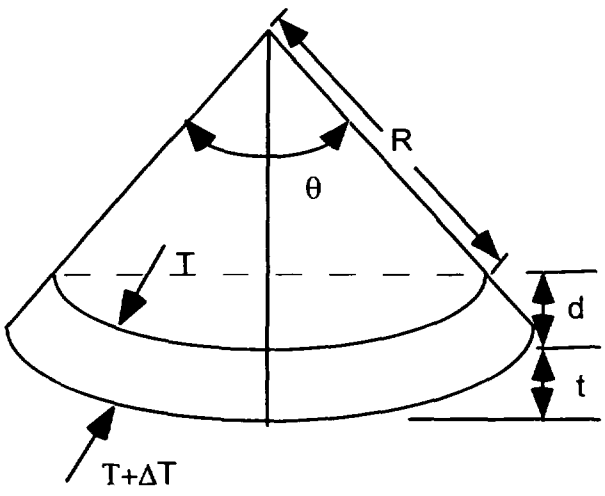

If the plate has clamped ends, then required bending moment to suppress the edge rotation is $M = \frac{\alpha \Delta T (1+\nu) D}{t}$, where D is a diameter, t is a thickness, and α is a thermal expansion coefficient. This

moment will produce biaxial bending stresses of $S = \frac{\alpha E \Delta T}{2(1-\nu)}$.

If we suppose the temperature of top of closure head as 93 °C and the temperature difference between top and bottom of the closure head as 10 °C, it will have biaxial compressive stresses of 21.32 MPa with a clamped edge condition. Considering ASME Code(Section III-NB) secondary stress limit of $3S_m$ (413.6 MPa) for SS304, above thermal stresses are acceptable. On the other hand, with a simply supported end condition and 10 °C temperature difference, the radius of curvature R is 3062.6 m and its angle θ is 0.215°. Thus the center of a plate will deform 0.54 cm downward. This needs to be verified to satisfy functional design requirement at a later time.

In addition to the deflection problem as explained above, thermal bowing of the closure causes edge moment at the top of the reactor vessel. The corresponding maximum circumferential stress at top of reactor vessel is calculated as:

$$\sigma_{limp} = \frac{E t^2 R(\Delta T)}{12(1-\nu^2)} \left[\frac{3(1-\nu^2)}{R^2 t^2}\right]^{3/4}$$

Assuming temperature difference between top and bottom surfaces of closure head as 10 °C yields maximum circumferential stress of 15.3 MPa which is about 7.4 percent of $1.5S_m$ for SS304.

While the above stresses/deflections corresponding to a 10 °C temperature gradient through the thickness appear acceptable, the edge rotation would have to be accommodated by the reactor structure support system. Larger temperature differences would produce correspondingly larger closure

deflections which may be functionally unacceptable or would require large clamping forces which would complicate the reactor support system design. Therefore it is desirable to maintain lower operating temperature and small temperature difference through the thickness of closure head.

4.2.3 Reactor Support Structures

The KALIMER reactor structure is supported by twelve radial support arms welded to the containment vessel flange as shown in Figure 8. When a thermal displacement of closure head and containment vessel flange occurs, reactor support structure should allow this thermal movement to prevent excessive thermal stresses from them. For example, if the temperature of closure head changes from room temperature of 20 °C to operating temperature of 150 °C, its radial thermal movement Δ can be calculated as:

$$\Delta = \alpha\,(\Delta T)\,D/2 = 1.273 \text{ cm}$$

Very large forces would be required to suppress this motion. Thus, support arms are preliminary designed to rest on Lubrite plates which permit radial thermal displacements by sliding while providing vertical support as shown in Figure 8. In addition, lateral seismic restraint is provided by the close fit of the support arm bolts within the radially slotted holes in the arms.

The structural analysis and thermal analysis of reactor support structures will be performed later when the design information of reactor support structures including operating conditions are available and the precise analysis for closure head are carried out.

4.3 Reactor Internal Structures

4.3.1 Support Barrel, Separation Plate, Liner, and Baffle Plate

Support barrel and thermal liner serve as the boundary between the hot pool and cold pool regions. The boundary is completed by the separation plate and baffle plate which span the gap between the liner and support barrel as shown in Figure 3, and block the sodium flow though slight sodium leakage flow may be allowed through the gaps in these components. Thus, the support barrel, separation plate, liner, and baffle plate form a box-ring structure serving as a barrier between hot sodium plenum and cold sodium plenum with the sodium inside the boxed structure remaining essentially stagnant.

Since the different sides of the box-ring structure would be exposed to the whole temperature rise through the core, it is anticipated that high thermal stresses would occur in these structures. Steady state heat transfer and thermal stress analyses were performed to estimate these stresses as explained in previous section. Results of these analyses are discussed in this section.

Support Barrel:

In this study, only the part of support barrel above the core exit elevation was analyzed applying the hot pool temperature of 533 °C on the inner surface and the cold pool temperature of 387 °C on the outer surface at elevation below the separation plate. Large temperature variation in radial direction occurred in the lower part of support barrel in this model which produced large thermal stresses particularly at the junction of the support barrel and the separation plate and in the bottom region of the model.

Figure 11 shows calculated temperature distribution near the junction of the support barrel and separation plate, and Figure 12 shows total stress intensity

contours in this region.. The calculated stress intensities were linearized giving linearized membrane plus bending stress intensities (P_m+P_b) of 441 MPa near junction of the separation plate and support barrel and 435 MPa at the bottom of support barrel. Since the temperatures in the support barrel exceed 427 °C, it is necessary to apply the limits in the ASME Code Case N-47. Considering $3S_m$ at 533 °C of 316 MPa which was obtained as $0.9S_y$ at operating temperature, above results is larger than $3S_m$ which is even larger than the limits for high temperature above 427 °C. Thus, the current elastic analysis results for support barrel fail to satisfy the limits of Code Case N-47. Therefore it becomes necessary to perform inelastic analysis for support barrel to investigate the design adequacy.

It should be noted, however, that thermal insulation will be provided to protect the support barrel from the core exit environment. This insulation, not included in the above heat transfer analyses, will reduce the temperature gradients through the support barrel with a corresponding reduction in thermal stresses. When more precise heat transfer analysis including insulation are performed, it will be necessary to check whether the application of Code Case N-47 is required. If so, T-1320 and T-1330 of Code Case N-47 need to be investigated with the analysis results to decide the necessity of detailed inelastic analysis.

Thermal Liner:

Thermal liner is in direct contact with hot pool sodium temperature of 533 °C at its inner surface below -3.1 m and above baffle plate location, and is supported by separation plate which is welded to the liner as shown in Figure 3. The inner surface of liner above hot sodium free surface was assumed to be adiabatic in the heat transfer analyses described above but needs to be

analyzed with radiation heat transfer between the liner and hot sodium surface and the layers of thermal insulation plates at a later time to reduce conservatism. The sodium inside the box-ring structure, which is supposed to be stagnant, transfers heat from support barrel to liner inner surface. The outer surface of liner transfers heat to reactor vessel only by the radiation above annulus sodium surface because convection heat transfer is assumed to be negligible. Below annulus sodium surface, annulus sodium conducts heat from liner to reactor vessel.

The liner experiences most significant temperature changes near hot pool sodium surface as expected. This leads to significant thermal stresses in both axial and circumferential directions which were calculated to be 148 MPa and 200 MPa, respectively. While these stress are below the ASME Section NB limit of $3S_m$ = 316 MPa, it is necessary to check the intents of Code Case N-47 at this location because of the high operating temperature of 533 °C which is above the Section NB limit of 427 °C for stainless steel. Substituting above results to the requirements of T-1320 and T-1330 in Code Case N-47 indicates that the current stress results failed to satisfy T-1320 and T-1330. Therefore detailed inelastic analyses are necessary.

Baffle Plate:

The heat transfer analysis results indicate small temperature variation through the baffle plate (10 °C). This produces maximum compressive axial stress of 50 MPa and compressive circumferential stress of 25 MPa near the junction of the baffle plate and liner. These stresses satisfy the elastic analysis tests of Code Case N-47. Therefore detailed inelastic analysis for baffle plate is not needed.

Separation Plate:

The separation plate is welded to the liner bottom and the support barrel wall at its outer and inner radius, respectively. Due to the assumption of stagnant sodium inside box structure, the temperature variation is not severe in separation plate except its both ends. The stresses in separation plate near support barrel have been discussed in previous section.

4.3.2 Upper Internal Structure

The KALIMER UIS, which is shown in Figure 13, is plug-in/out type safety-related structure. The UIS lower assembly is governed by the thermal loads rather than mechanical loads, which are expected to be small. While detailed design data and thermal hydraulic results are not available, simple method of thermal stress evaluation for the UIS structures considering steady state operation and thermal transients are described below.

Steady State Operation (thermal striping):

Since the UIS bottom plate is approximately 90 cm above the core outlet and the shroud tube is 5 cm above the core exit, significant thermal striping loads during steady state operation due to the mixing of the sodium jets from different core assemblies with different velocities and temperatures are expected to occur on these structures.

1) Striping Loads

The thermal striping calculations use a combination of thermal hydraulic tests and analyses and involve 1) estimation of the core exit striping potential from core thermal hydraulic analyses, 2) estimation of the coolant striping attenuation in transit to the component surface from appropriate mixing tests,

3) calculation of the metal temperature distribution history using experimental film coefficients and heat transfer analyses, and 4) calculation of the component thermal stress distribution/history using stress analysis.

The test and analysis information required for striping stress calculation is not presently available for KALIMER. Therefore the KALIMER UIS assessment is based upon the assumed condition which is based on the experience and ALMR data.

The maximum differences in the core exit coolant temperatures between adjacent fuel assemblies is the maximum striping a component may experience and is termed striping potential. This difference is generally larger than the increase in the bulk coolant temperature through the core because of the uncertainty factors. The maximum striping potential generally results from difference between the coolant temperature from a control assembly and an adjacent fuel assembly. This was assumed as 200 °C which is close to the ALMR value.

The coolant striping at the UIS component surfaces will be lower than the core exit striping potential because of the coolant mixing in transit. This striping attenuation is best estimated in mixing tests with prototypical geometry and flow conditions. Depending on the relative velocities, flow rates, geometry in the mixing region and the distance of the component from the core exit plane, the attenuation may vary range from about 20 to 80% based upon tests performed in water. The striping attenuation in sodium is known to be about 20% larger than that in water because of the higher thermal conductivity of sodium. Since such tests are not available and the objective of present analysis is to examine the general behavior of bottom plates under striping

loads, the striping potential is used for conservatism. The four cycles of sinusoidal striping load with 1 Hz frequency used in this study is shown in Figure 14.

II) Heat Transfer Analysis

Thermal stresses will depend on the depth of penetration of striping in the metal. For the UIS components of interest, this may be conservatively estimated by one-dimensional heat transfer analysis for a flat plate or a tubular component. The striping reduction across the surface film depends on the film coefficient and the striping frequency. The dynamic film coefficients in the striping environment are generally not known. Therefore parametric analyses are performed with film coefficient values of 28400, 284000, and 454400 J/sec-m^2-°C. The frequency effects on the striping penetration were studied with 0.5, 1, and 2 Hz striping frequencies.

One dimensional heat transfer analysis was performed using ANSYS finite element code with PLANE55 elements. Both Stainless Steel 316 and Inconel 718 were analyzed with their material properties at 533°C which is the average temperature of striping loads. The density, specific heat, and thermal conductivity for SS316 are 7746 Kg/m^3, 576.1 J/Kg-°C, and 21.3 W/m-°C, and the density, specific heat, and thermal conductivity for 1718 are 8039 Kg/m^3, 496.4 J/Kg-°C, and 18.52 W/m-°C respectively. Striping loads were applied on one side of the plate and the other side was held at 533 °C .

Thermal stresses depend on the depth of penetration of striping in the metal plate or the tubular component. The depth of striping penetration for striping frequencies of 0.5, 1, and 2 Hz are shown in Figure 15. Figure 16 shows the striping reduction for three values of film coefficients at the metal surface

(28400, 284000, and 454400 J/sec-m^2-°C). Both results are obtained using SS316 and striping history results are enveloped to show the depth of penetration of striping. Analyses results indicate that the striping reduces to small values within about 0.3 cm of the surface and essentially disappears within 0.7 cm of the surface. Since the predicted striping stresses are greater than SS316 capacity, it is necessary to introduce an I718 lining plate to prevent striping load to be delivered to SS316 UIS lower plate. The thickness of I718 lining plate and the thickness of I718 shroud tube are preliminary determined as 0.6 cm.

As striping frequency becomes high, striping penetration depth decreases and film coefficient greater than 284000 J/sec-m^2-°C does not affect striping attenuation. On the other hand film coefficient of 28400 J/sec-m^2-°C reduces striping by about 40 % compared to the case with 284000 J/sec-m^2-°C. Figure 17 shows comparison of resultant striping in the metals for both SS316 and I718. It can be seen that there are no big differences between the results for the two materials. Figure 18 shows the maximum striping slope through metal thickness at certain time.

III) Striping Stresses

Based on the above analyses, striping stresses may be conservatively estimated by assuming the metal surface striping to be 100% of the local coolant striping even though the actual metal surface striping may be much smaller than the local coolant striping, and a linear reduction to zero striping within 0.13 cm of the surface. The corresponding striping stress amplitude could be calculated using the following formula as explained in Appendix 1:

$$\sigma_{striping} = E\alpha\,(1 - 0.13/t)\,(T_{striping}/2)/(1-v)$$

where t is the component wall thickness and $T_{striping}$ is the peak-to-peak metal striping at the surface. Young's modulus, Poisson's ratio, and thermal expansion coefficient for I-718 at 533 °C are 171.7 GPa, 0.273, and 14.35×10^{-6}/°C. Peak to peak metal striping at surface from above analysis is about 190°C and the thickness of I-718 liner plate and shroud tube are 0.6 cm. Applying these values results in striping stress 252.2 MPa which is much less than the yield stress 882.3 MPa. Actual stresses would be smaller because of the nonperiodic temperature variation, and because of the nonuniform temperature distributions which would lead to accommodation of some of the thermal expansions at a point by the surrounding material at different temperatures.

Thermal Transient:

Assume that the peak fuel assembly core exit transient temperature for the RVACS transient immediately after the reactor and pump trip is approximately 5 ~ 10 °C per second near the core exit. The rate of temperature reduction will decrease significantly at the downstream components due to thermal inertia of hot pool and the lack of mixing. Thus, only the UIS bottom structures including instrument support posts, the control rod driveline/shroud tubes, and the UIS lower plate are expected to experience significant thermal shock. The response of these components to postulated thermal transient was evaluated using one dimensional heat transfer analyses and conservative methods of calculating thermal stresses.

One dimensional heat transfer analyses have been performed using ANSYS with two dimensional plane thermal element(PLANE55) and SS316 material properties. Thermal transient of 5°C/sec decreasing linearly from 560 °C to

390 °C, as shown in Figure 19, was applied on one side of the model while the temperature on the other side was held at 533 °C which is the hot pool temperature. As discussed in previous section, film coefficient of 284000 J/sec-m^2-°C has been assumed and compared to the analysis results for 28400 and 454400 J/sec-m^2 °C. Figures 20, 21, and 22 show the temperatures at several time steps versus distance from surface for each values of film coefficient. Results shows that the film coefficient 454400 J/sec-m^2 °C which is 1.6 times assumed value 284000 J/sec-m^2 °C does not affect the temperature gradient through metal surface and the smaller film coefficient produce slightly milder temperature gradient. As shown in Figure 13, in addition to the 0.6 cm I718 liner, a 1.2 cm SS316 thermal liner was introduced to alleviate the thermal shock upon 2.5 cm SS316 UIS bottom plate. Based on Figures 20, 21, 22, the maximum temperature differences across the 0.6 cm I718 liner, 1.2 cm SS316 liner, and 2.5 cm UIS bottom plate within 40 seconds are 71 °C, 76 °C, and 32 °C, respectively.

With these temperature gradients across each liner and plate, corresponding thermal stresses were calculated conservatively as follows. When a plate of thickness h in the xy plane is loaded by linear temperature gradient ΔT through the thickness and is clamped at ends to suppress bending completely, strains in the plane of the plate are zero, and the maximum biaxial bending stresses are given by:

$$\sigma_x = \sigma_y = \frac{E\alpha\Delta T}{2(1-\nu)}$$

where ΔT is through-the-thickness linear temperature variation. Young's modulus, thermal expansion coefficient, Poisson's ratio, and yield stress for

SS316 are 163 GPa, $20x10^{-6}$/°C, 0.3, and 119 MPa, and Young's modulus, thermal expansion coefficient, Poisson's ratio, and yield stress for I718 are 176.4 GPa, $15.7x10^{-6}$/°C, 0.27, and 899 MPa at 450 °C which is close to the average temperature of transient. Substituting temperature differences of 71, 76, and 32°C into above equation yield 134.9 MPa, 177 MPa, and 74.5 MPa respectively. Thermal stress in I718 liner is small compared to the yield stress and the thermal stress in SS316 liner and UIS bottom plate satisfy allowable stress 321 MPa which is evaluated three times of 90 percent of yield stress.

Figure 23 shows temperature gradient through metal surface within first 20 seconds against the more severe thermal transient decreasing at 10 °C/sec from 560 °C to 390 °C. The maximum temperature differences through 0.6 cm I718 liner, 1.2 cm SS316 liner, and 2.5 cm UIS bottom plate within 40 seconds are 92 °C, 75 °C, and 13 °C respectively and corresponding thermal stresses are 174.8 MPa, 174.7 MPa, and 30.3 MPa each. These stresses are within the allowable stress limits as discussed before and the current conceptual design adopting I718 liner to absorb striping loads and SS316 thermal liner to mitigate thermal shock beneath UIS bottom plate is considered to be adequate with postulated thermal transient loadings. Figure 24 shows the temperature difference using I718 and the difference with the case of SS316 is within 1 percent.

Control rod shroud tube, which is made of 0.6 cm I718, attached to the UIS bottom will undergo maximum temperature difference of 71 °C and 92 °C for 5 °C/sec and 10 °C/sec transients respectively. Corresponding thermal stresses are calculated as 134.9 MPa and 174.8 MPa and these are within 20 percent of yield stress.

References

1. 액체금속로 요소기술개발, KAERI/RR-1528/94
2. ASME B&PV Code, Code Case N-47, ASME, New York, 1992
3. 유봉, 구경회, 이재한, "KALIMER 면진 개념설계/해석", KAERI/TR-697/96, 한국원자력연구소, 1996
4. ANSYS, Version 5.2, Swanson Analysis Systems Inc., USA

Appendix 1. Striping Stress Calculation

$$L_1 = L(1+\alpha T_1) \quad (1)$$

$$L_2 = L(1+\alpha T_2) \quad (2)$$

$$\sigma_1 = \frac{E}{1-\nu}\frac{L_1 - L_0}{L_1} \quad (3)$$

$$\sigma_2 = \frac{E}{1-\nu}\frac{L_2 - L_0}{L_2}$$

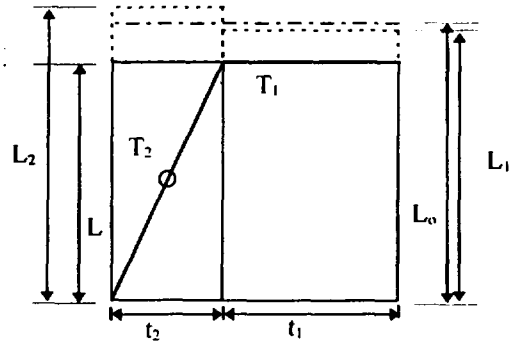

As shown in the above figure, the right hand rectangle has constant temperature of T1 and the left side rectangle has a linear temperature variation from T_b to T_1 so that the average temperature is T_2. Since there is no external force, using $\Sigma F=0$ leads to

$$\sigma_1 t_1 + \sigma_2 t_2 = 0$$

Substituting equations (1) - (3) into above equation leads to $L_0 = \dfrac{t}{\dfrac{t_1}{L_1} + \dfrac{t_2}{L_2}}$.

Now maximum stress σ_2 in left rectangle is calculated as :

$$\sigma_2 = \frac{E}{1-\nu}\frac{L_2 - L_0}{L_2}$$

$$= \frac{E}{1-\nu}\frac{L_2 - \dfrac{tL_1L_2}{t_1L_2 + t_2L_1}}{L(1+\alpha T_2)}$$

$$= \frac{E\alpha(T_2 - T_1)}{1-\nu}\frac{t_1}{t}\frac{1}{1+\alpha\left(\dfrac{t_1T_2 + t_2T_1}{t}\right)}$$

From above, the last term in right hand expression is considered as $\dfrac{E\alpha(T_2 - T_1)}{1-\nu}\dfrac{t_1}{t}$ since $\alpha\left(\dfrac{t_1T_2 + t_2T_1}{t}\right)$ is the order of 10^{-3} or 10^{-4}. (Note that 1/1.0001 = 0.9999 ≅ 1.)

And substituting $T_2 - T_1 = (T_b - T_a)/2$ results in $\sigma_2 = \dfrac{E\alpha}{1-\nu}\left(1 - \dfrac{t_2}{t}\right)\dfrac{T_b - T_a}{2}$

where t is the component thickness and t_2 is the thickness having linear temperature variation from T_b to T_a.

Table 1 Reactor Vessel Design Data (Tentative)

Vessel Outer Diameter	1105.0 cm
Vessel Shell length	1420 cm
Main Cylinder Wall Thickness	5.0 cm
Bottom Head Thickness	5.0 cm
Construction Material	Type 316 Stainless Steel
Design Temperature	533 °C
Design Pressure	0.14 MPa

Table 2 Containment Vessel Design Data (Tentative)

Vessel Outer diameter	1150.0 cm
Vessel Length	
Main Shell, Including Top Flange and Bottom Head	1538.5 cm
Main Cylinder Wall Thickness	2.5 cm
Bottom Head Thickness	2.5 cm
Construction Material	2-1/4Cr-1Mo Low Alloy Steel
Design Temperature	TBD
Design Pressure	0.14 MPa

Table 3 Material Properties for Thermal Analyses (SS 316, 2.25Cr-1Mo, Sodium)

(a) SS 316

Temp (°C)	Thermal Expansion α (m/m/°C)	Density ρ(kg/m³)	Thermal Conductivity k(J/sec.m.°C)	Poisson's Ratio, ν	Young's Modulus (GPa)	Specific Heat c(J/Kg.°C)
-17.8	1.4753E-05	7861.12	12.69997			448.8464
37.78	1.5270E-05		13.65573	0.27	163	472.3338
93.33	1.5749E-05		14.59568			492.4997
148.9	1.6190E-05		15.51962			509.7058
204.4	1.6595E-05		16.42733			524.3136
260	1.6968E-05		17.31864			536.6844
315.6	1.7308E-05		18.19334			547.1799
371.1	1.7619E-05		19.05122			556.1616
426.7	1.7902E-05	7780	19.89211			563.9909
482.2	1.8159E-05	7757	20.71578			571.0294
537.8	1.8393E-05	7735	21.52206	0.304	156.65	577.6385
593.3	1.8604E-05		22.31074			584.1798
648.9	1.8795E-05		23.08162			591.0148
704.4	1.8968E-05		23.8345			598.505
760	1.9125E-05		24.56919			607.0118
815.6	1.9268E-05		25.28549			616.8969

(b) 2.25Cr-1Mo

Temp (°C)	Thermal Expansion α (m/m/°C)	Density ρ(kg/m³)	Thermal Conductivity k(J/sec.m.°C)	Poisson's Ratio, ν	Young's Modulus (GPa)	Specific Heat c(J/Kg.°C)
21.11	1.1610E-05		36.18473			
37.78	1.1700E-05		36.3509	0.265		
93.33	1.2060E-05		36.8702			
148.9	1.2420E-05		37.22332			
204.4	1.2726E-05		37.22332			
260	1.3014E-05		37.03638			
315.6	1.3284E-05		36.51708			
371.1	1.3500E-05		35.8316			
426.7	1.3716E-05		34.95918			
482.2	1.3914E-05		34.10753			
537.8	1.4076E-05		33.06894	0.304	156.65	
593.3	1.4220E-05		32.03034			
648.9	1.4346E-05		31.15792			
704.4	0.0000E+00		29.7662			
760	0.0000E+00		27.00353			
815.6	0.0000E+00		26.48423			0

(c) Sodium

Temp (°C)	Thermal Expansion α (m/m/°C)	Density ρ(kg/m^3)	Thermal Conductivity k(J/sec.m.°C)	Specific Heat c (J/Kg.°C)
-17.8		954.13	94.01382	1447.446
37.78		941.394	90.79922	1415.7
93.33		928.658	87.65702	1386.808
148.9		915.923	84.58724	1360.771
204.4		903.187	81.58987	1337.589
260		890.452	78.66491	1317.262
315.6		877.716	75.81236	1299.789
371.1		864.981	73.03222	1285.171
426.7		852.245	70.3245	1273.407
482.2		839.509	67.68918	1264.499
537.8		826.774	65.12628	1258.445
593.3		814.038	62.63578	1255.245
648.9		801.303	60.2177	1254.901
704.4		788.567	57.87203	1257.411
760		775.832	55.59877	1262.776
815.6		763.096	53.39792	1270.995

Table 4 Estimated Structural Weights of KALIMER Structures

Components	Weight (Ton)
Reactor Vessel	200
RV Liner	30.4
Support Barrel	40.4
Inlet Plenum	57.3
Baffle Plate	11.2
Separation Plate	45.6
Core Support	23.7
Core	156.4
Sodium	750
Total	1315

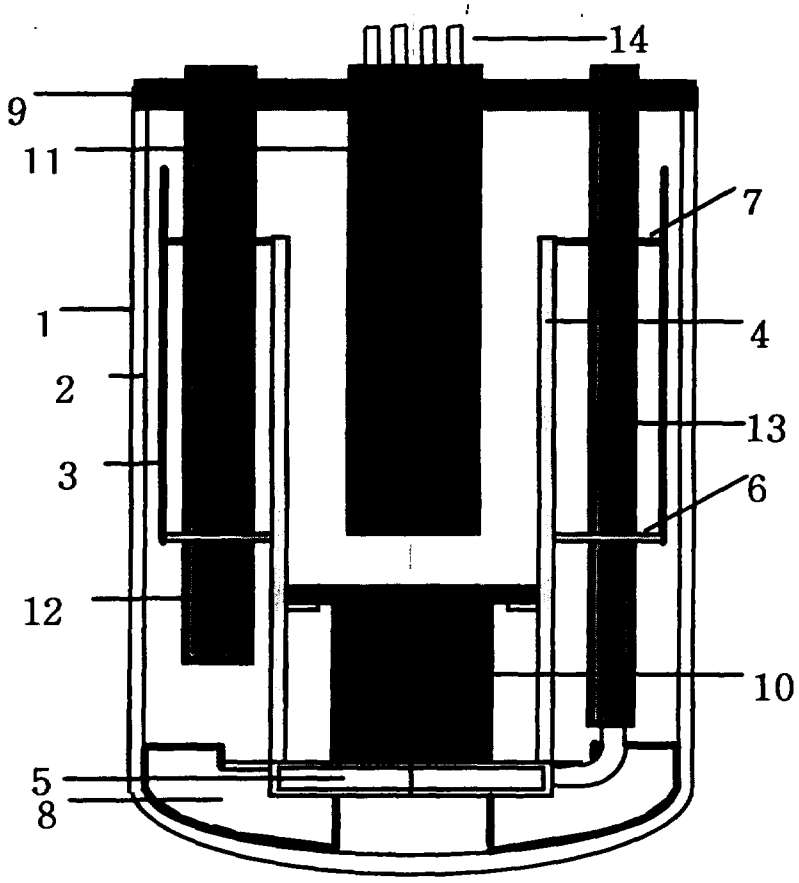

Figure 1 Schematic of Reactor Structures and Components

(Note:1. Containment Vessel 2. Reactor Vessel 3. RV Liner 4. Support Barrel 5. Inlet Plenum 6. Separation Plate 7. Baffle Plate 8. Core Support 9. Closure Head 10. Core 11. Upper Internal Structure 12. Intermediate Heat Exchanger 13. EM-Pump 14. Control Rod Drive)

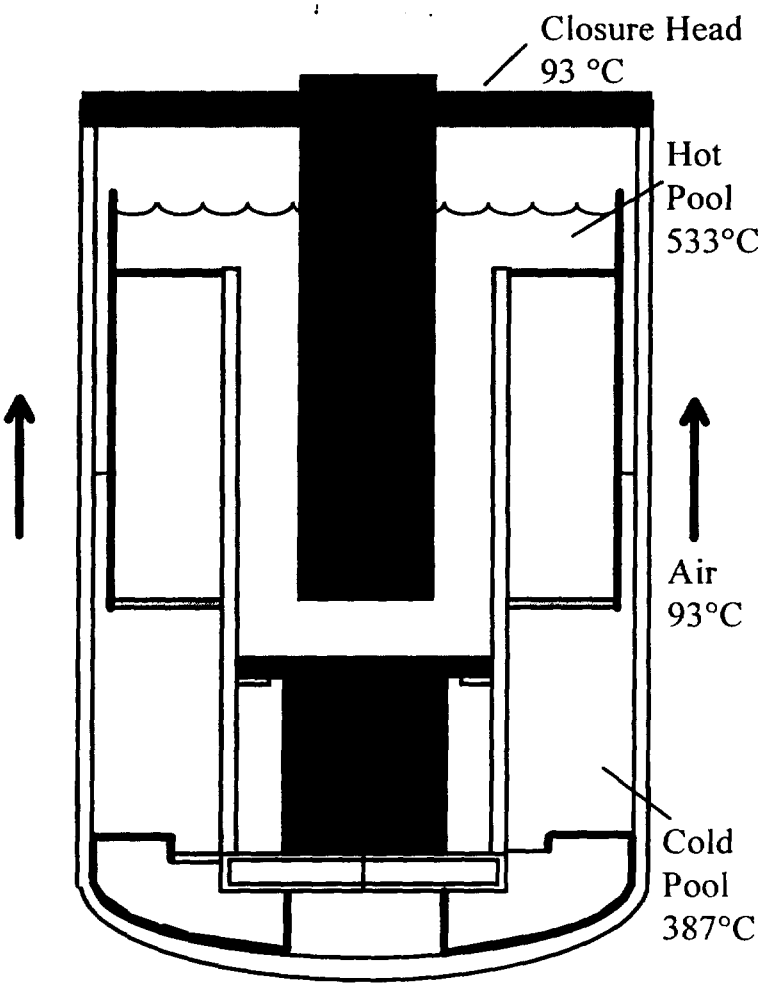

Figure 2 Predicted Steady State Temperatures of KALIMER

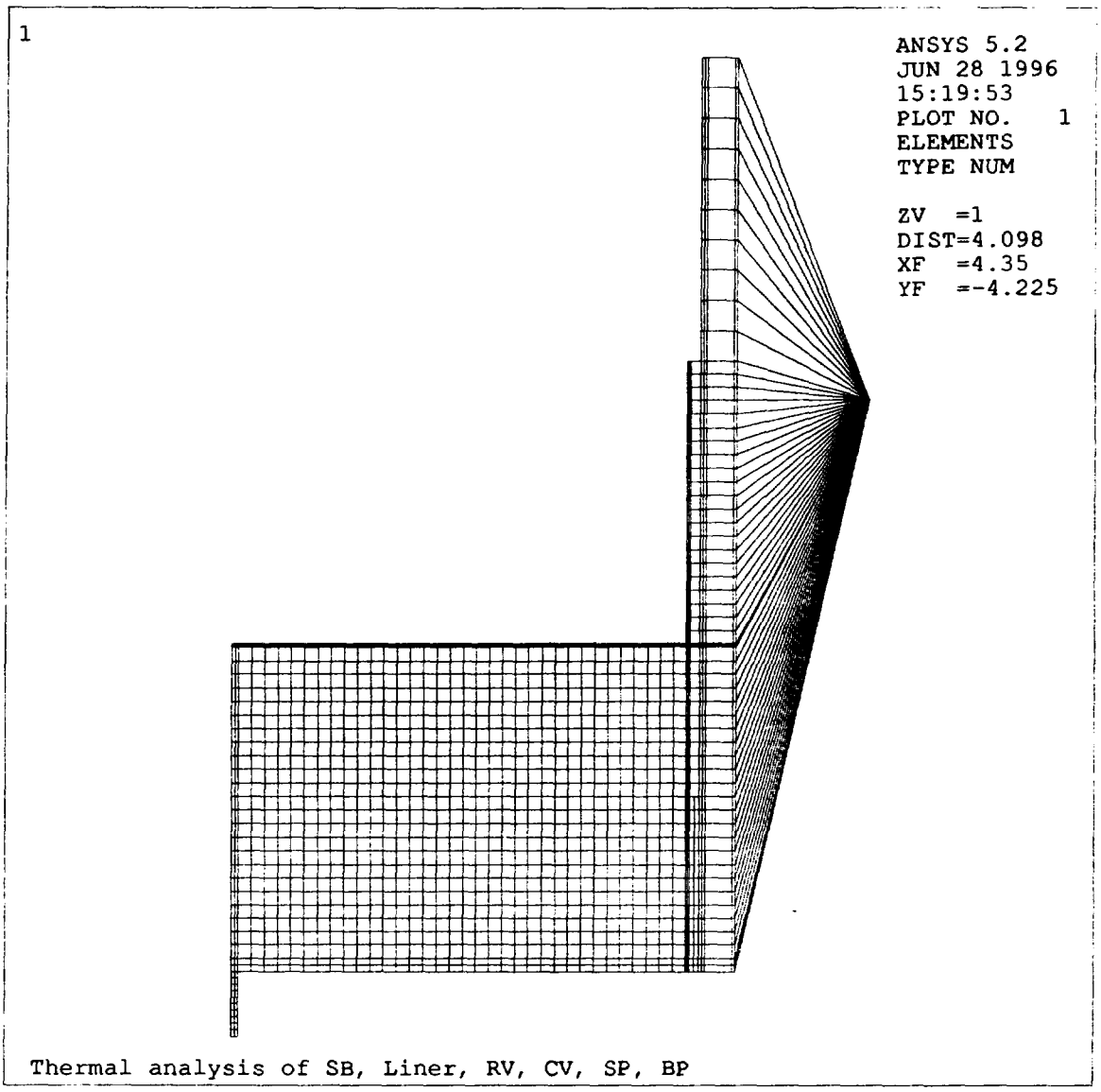

Figure 3 ANSYS Heat Transfer Analysis Model for KALIMER Structures

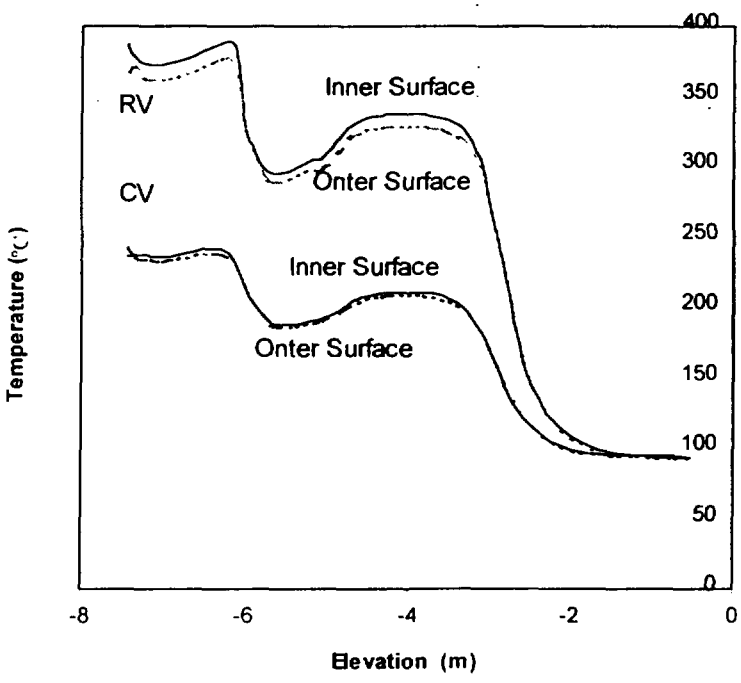

Figure 4 RV and CV Temperature Distributions (Normal Operation)

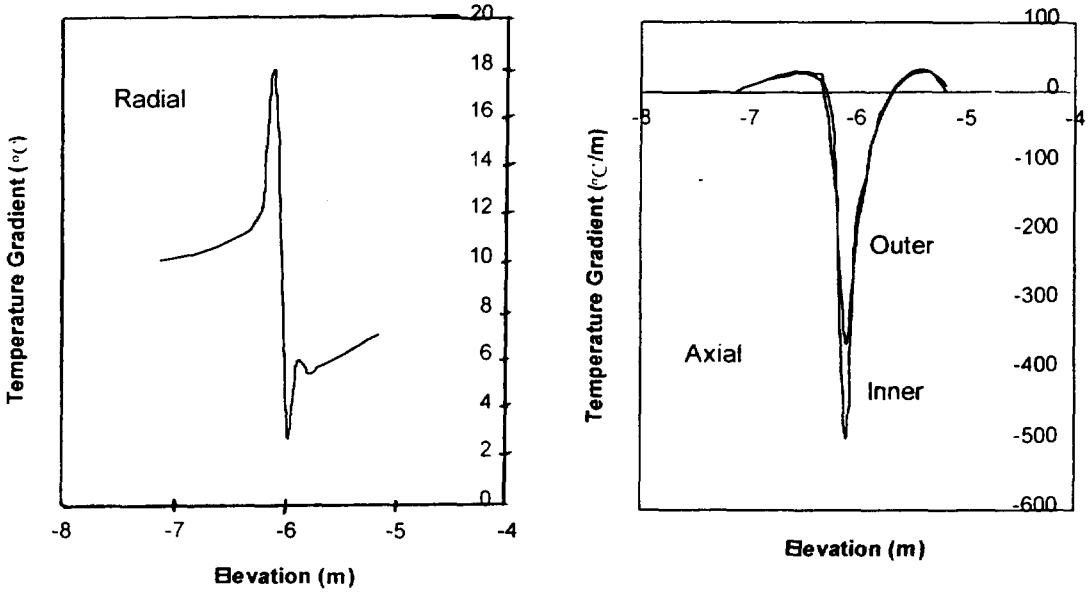

Figure 5 Reactor Vessel Temperature Gradients Near Sodium Surface

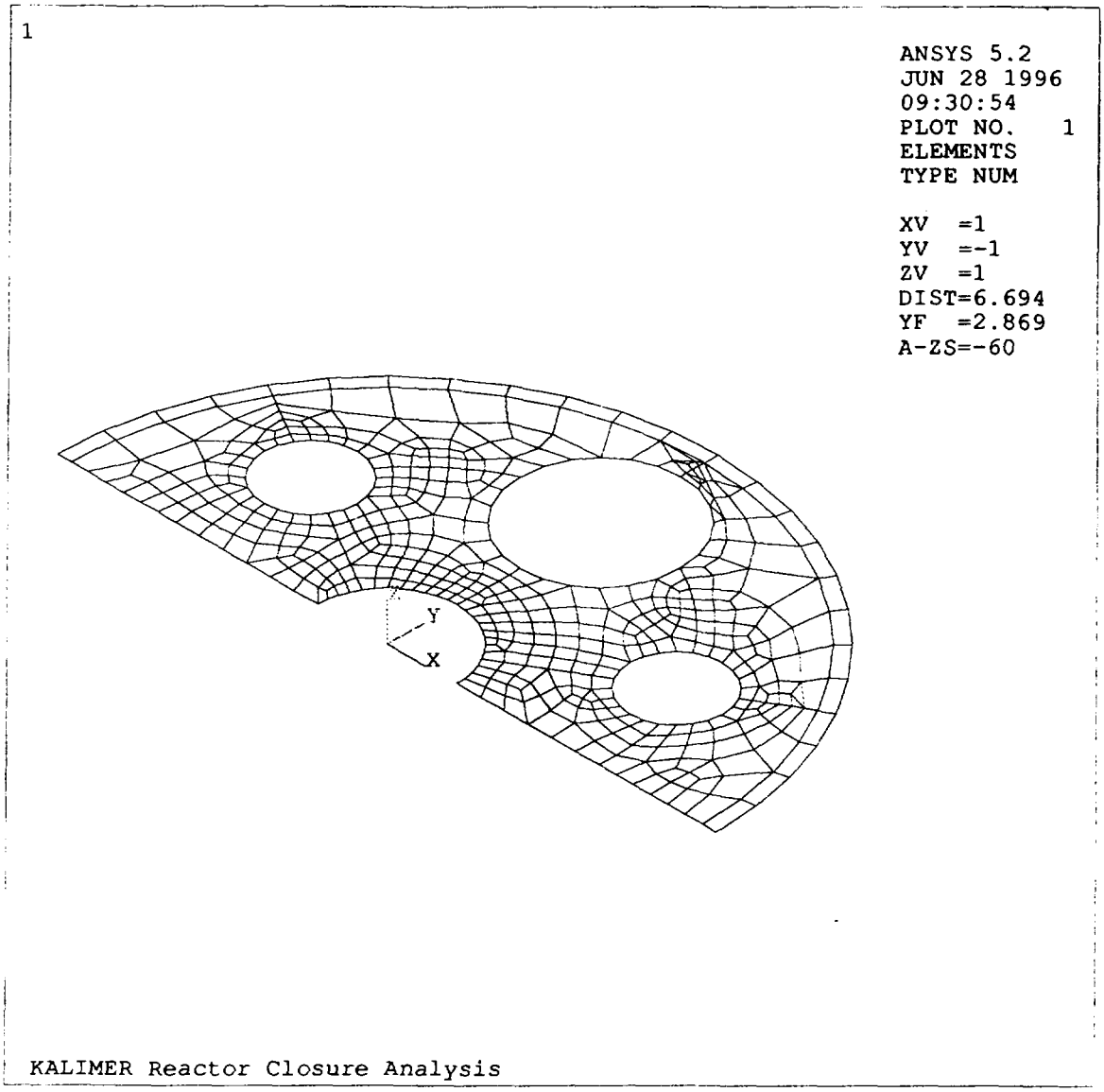

Figure 6 Closure Head Finite Element Analysis Model

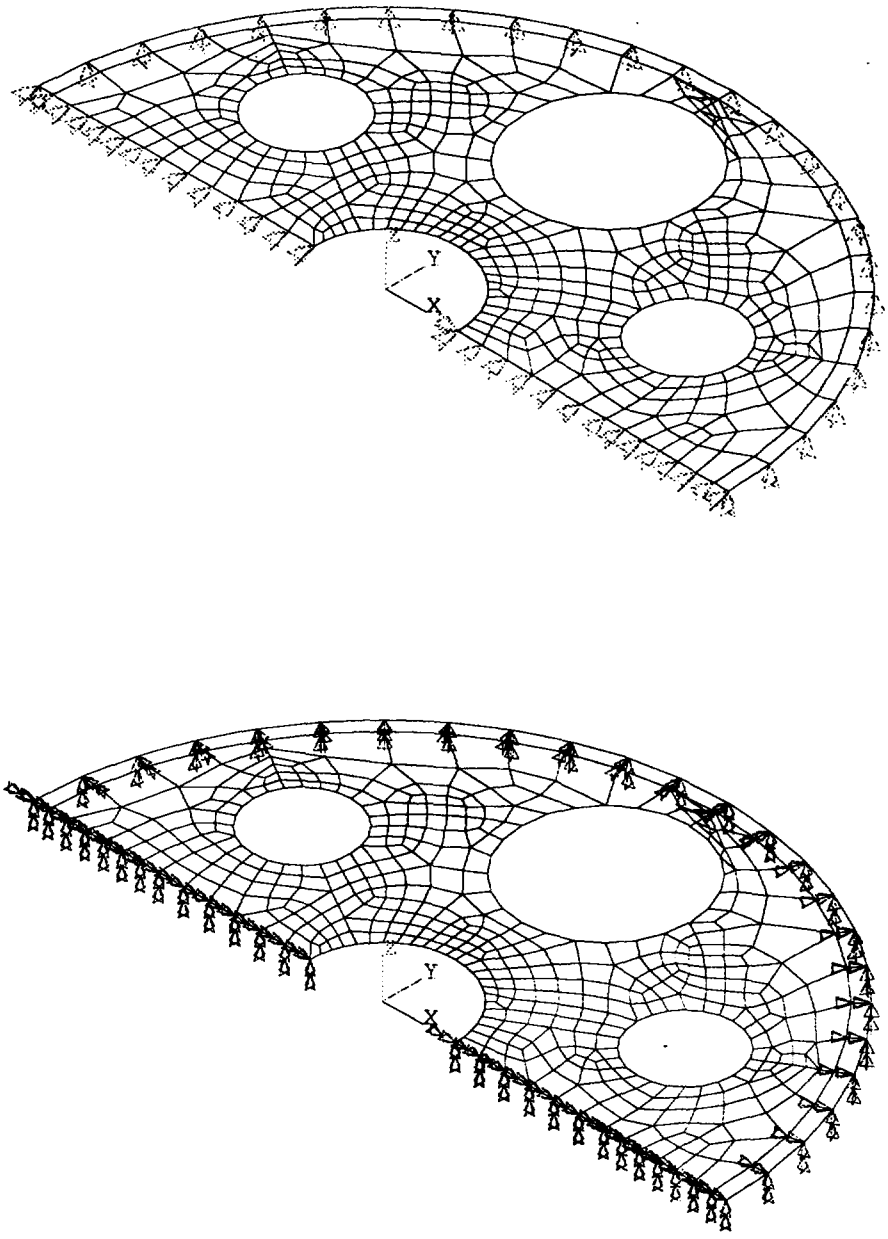

Figure 7 Boundary Conditions of Closure Head FEM Model

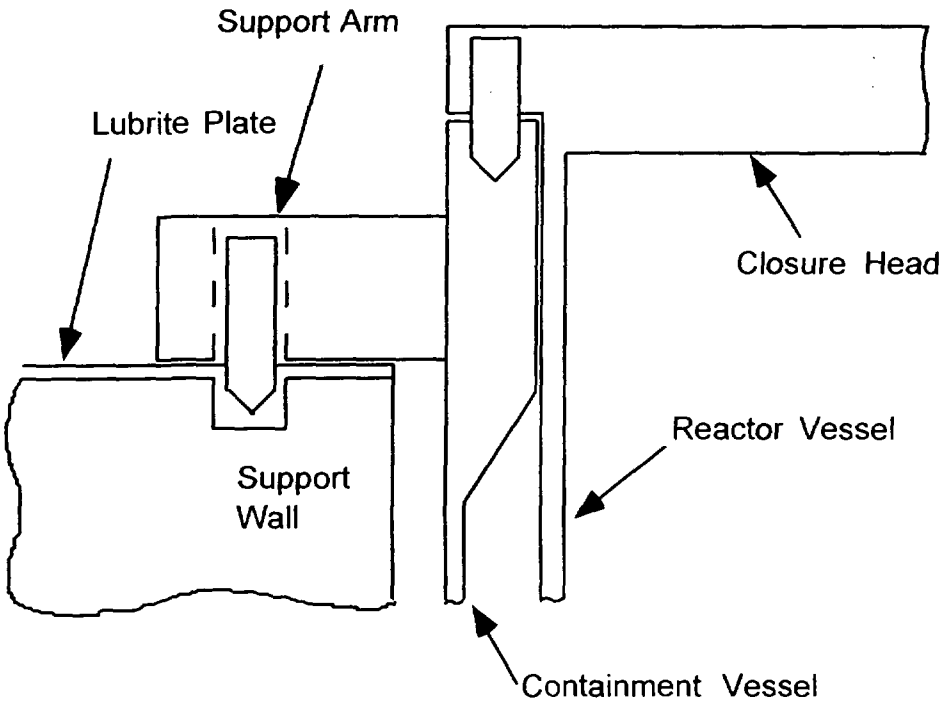

Figure 8 Schematic of Reactor Support System

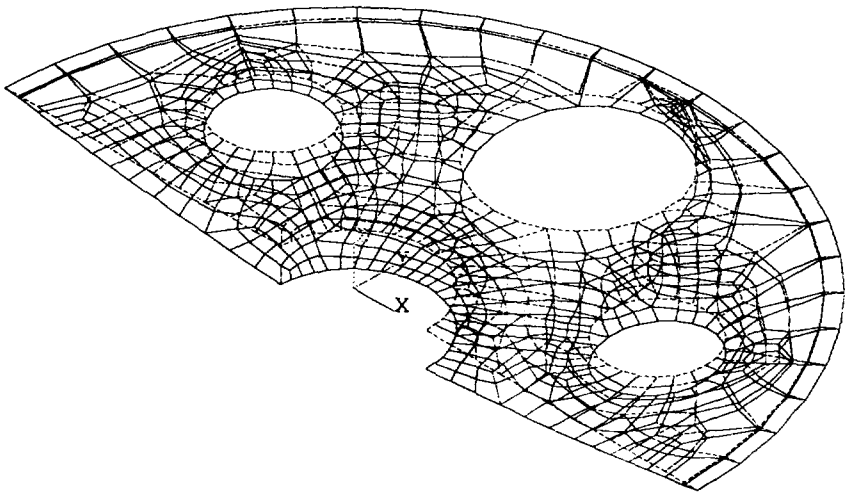

Figure 9 Deformed and Undeformed Shapes of Closure Head

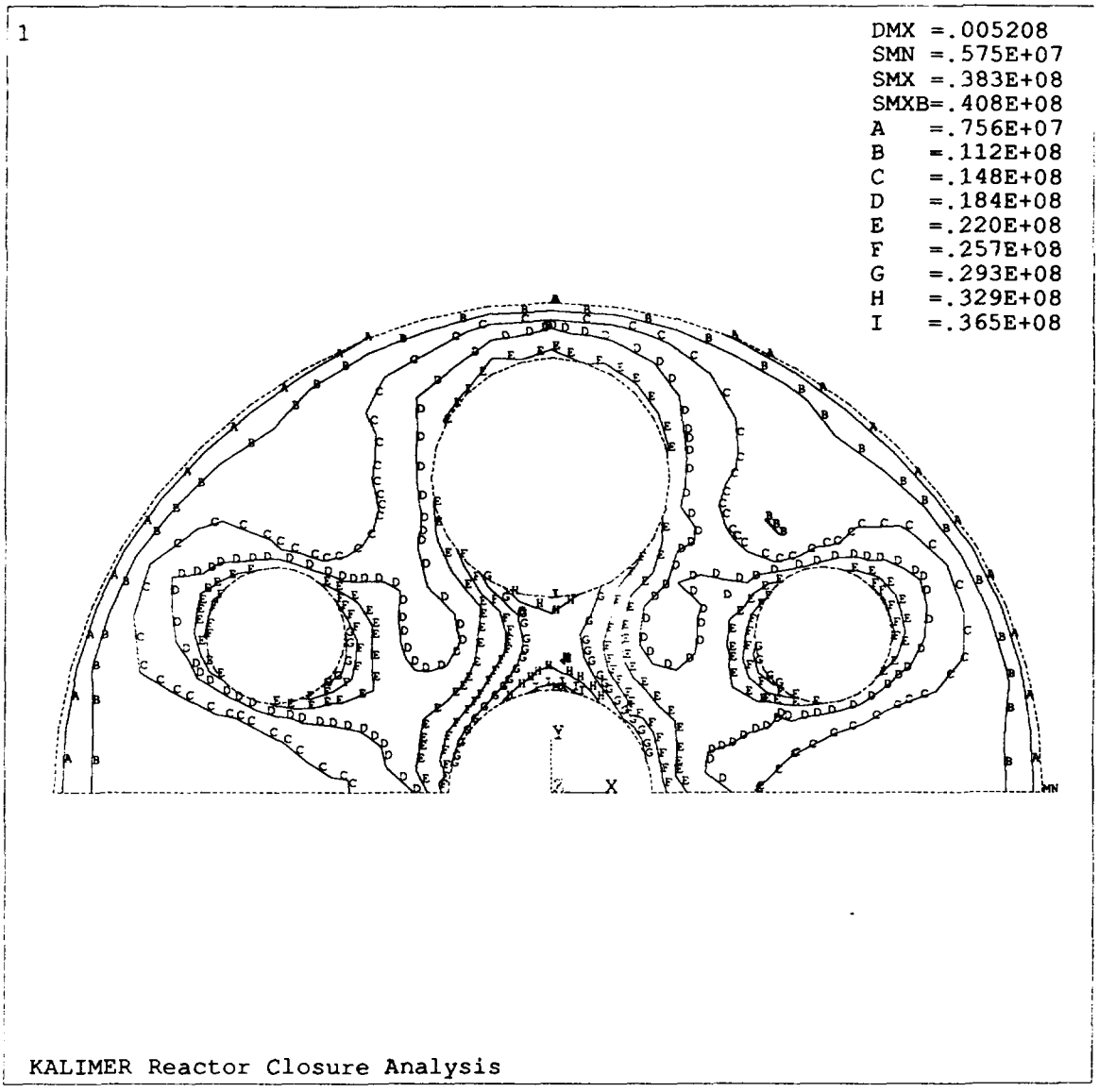

Figure 10 Stress Intensity Contour of Closure Head

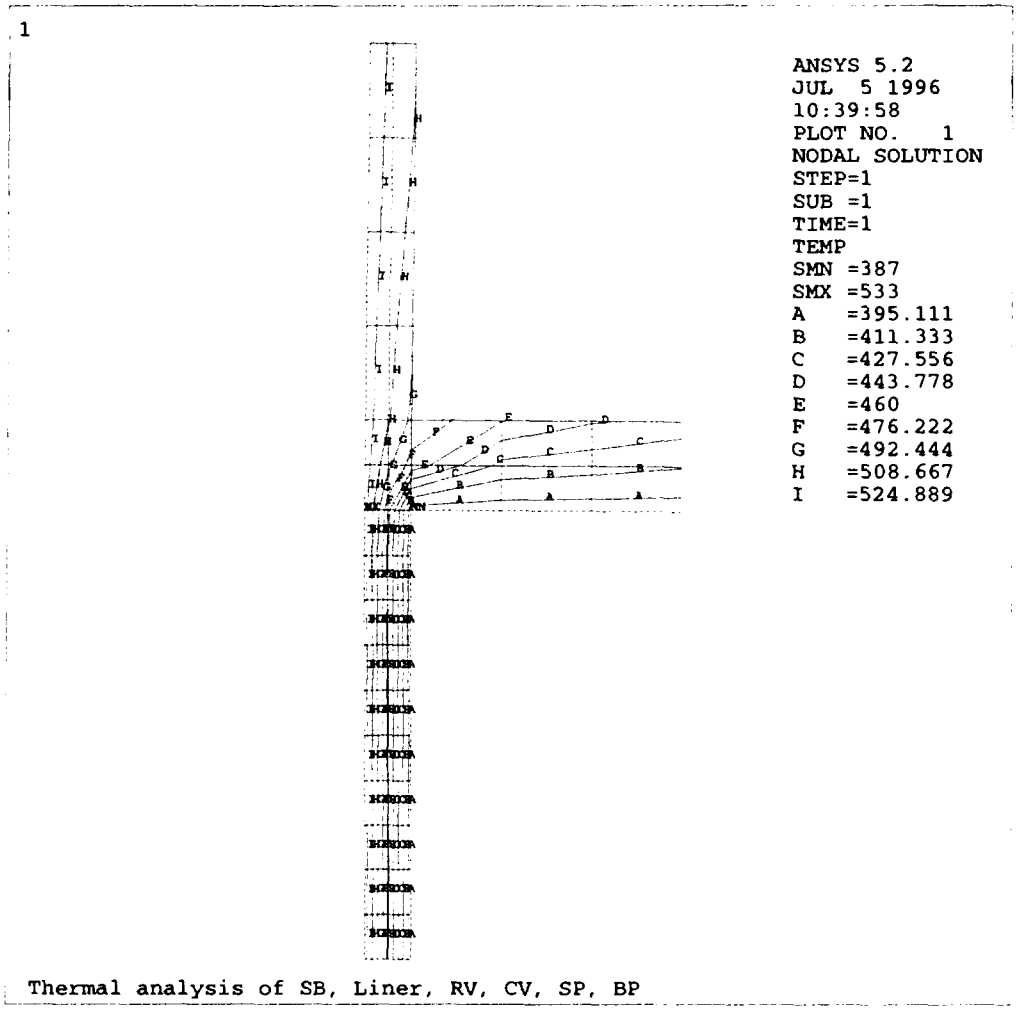

Figure 11 Temperature Distribution Near Junction of Support Barrel and Separation Plate (Normal Operation)

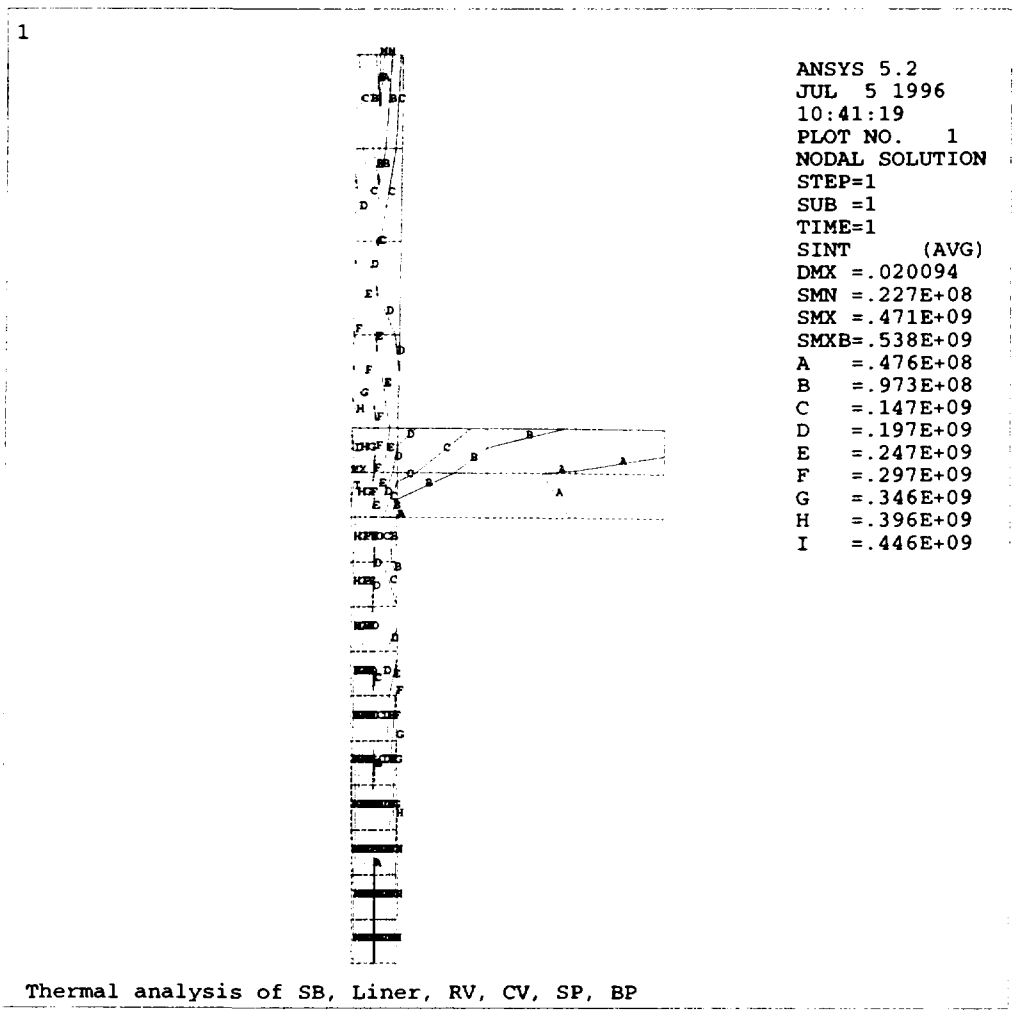

Figure 12 Stress Intensity Contour near Junction of Support Barrel and Separation Plate (Normal Operation)

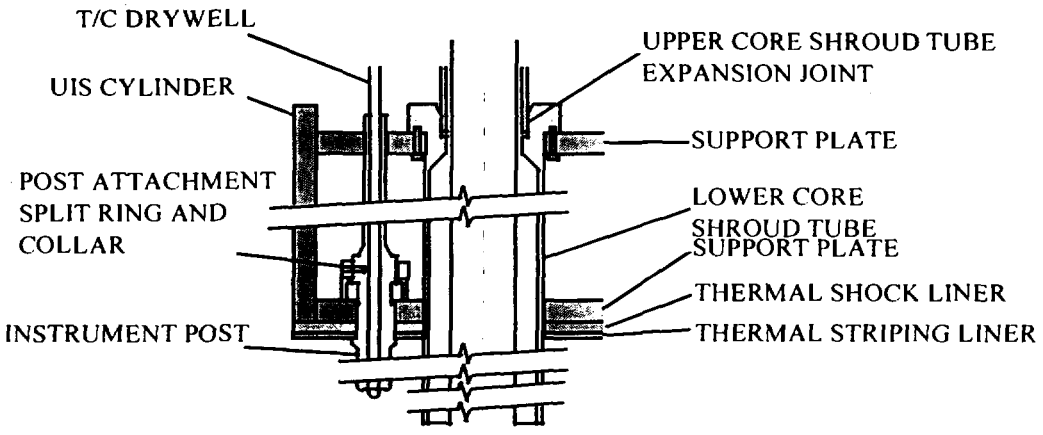

Figure 13 Schematic of Upper Internal Structures

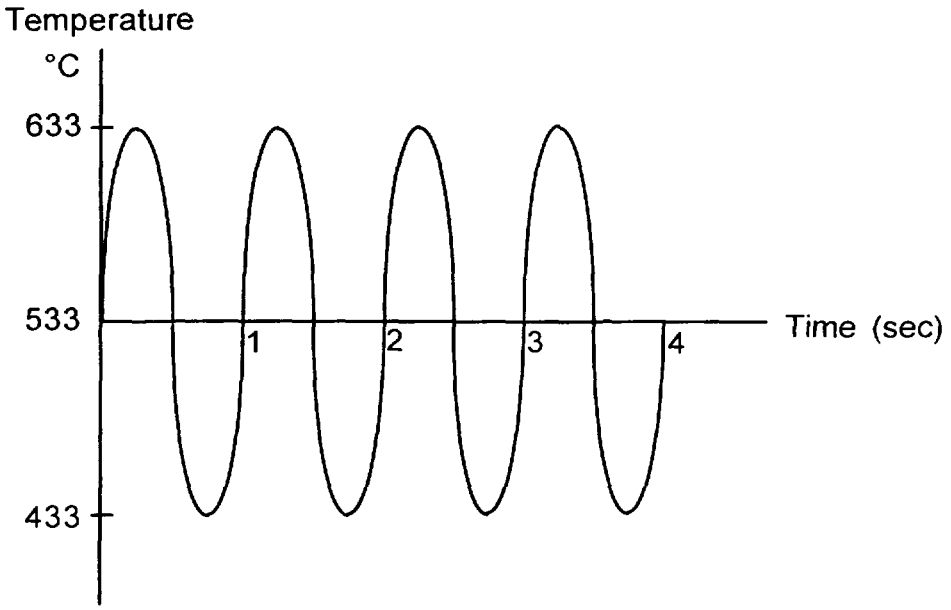

Figure 14 Striping Loads for UIS (Steady State Operation)

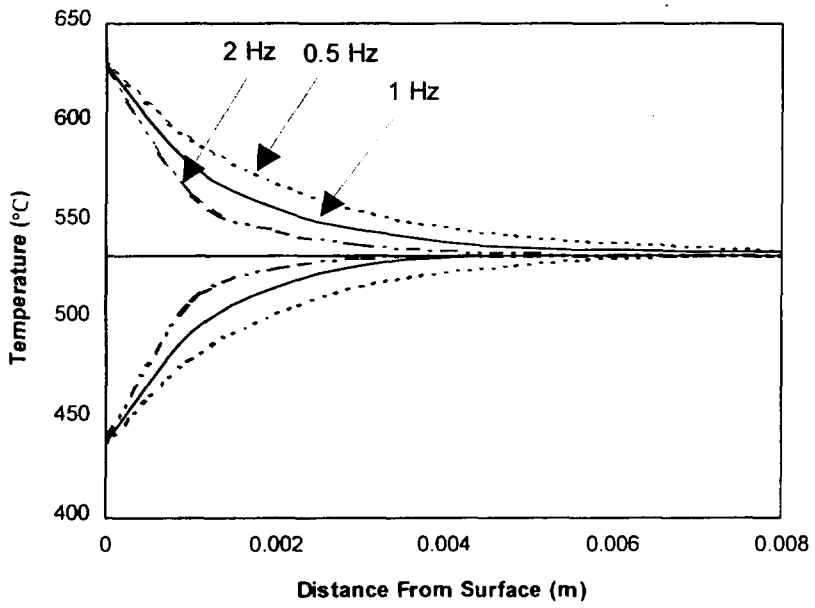

Figure 15 Striping Penetration with Various Striping Frequencies
(SS316 Plate)

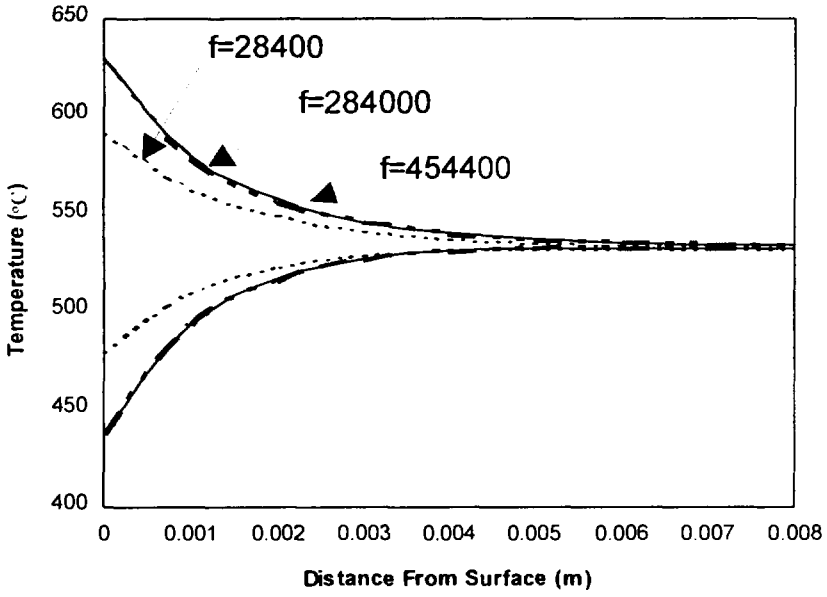

Figure 16 Striping Penetration with Various Film Coefficients
(SS316 Plate : f [J/sec.m^2.°C])

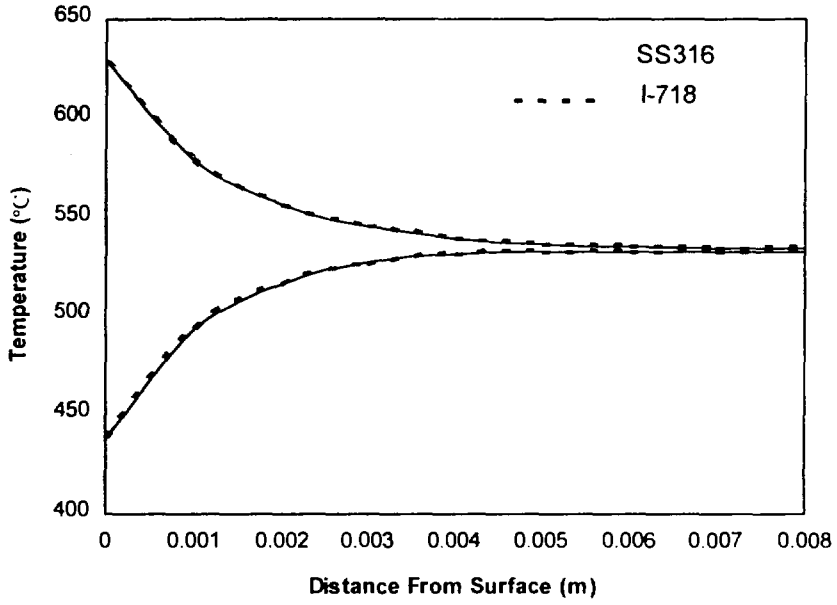

Figure 17 Comparision of Striping Penetration Between SS316 and I-718

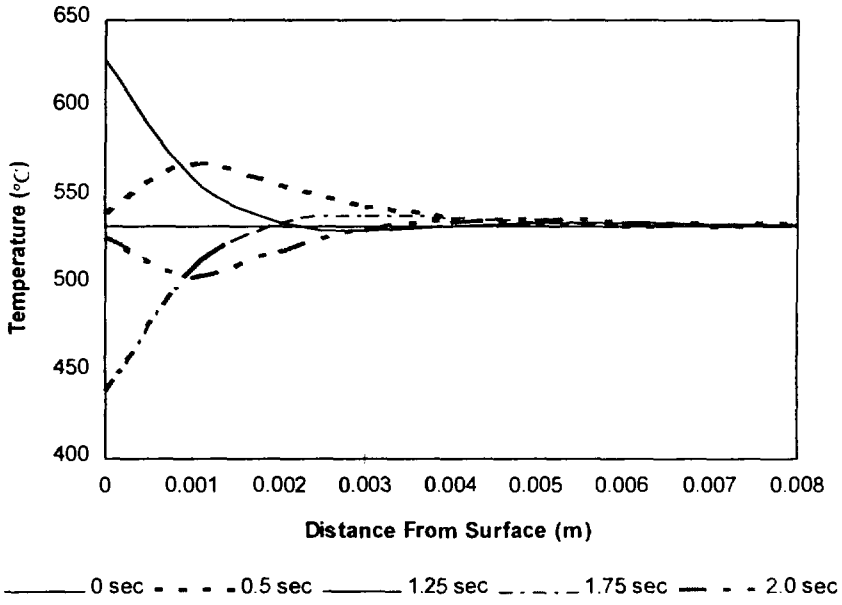

Figure 18 Instantaneous Striping Penetration in SS316 Plate

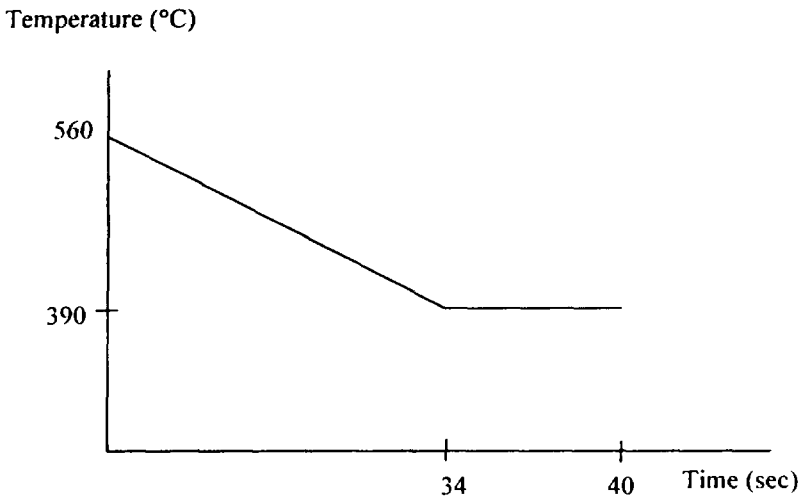

Figure 19 Thermal Transient Load for UIS (5 °C/sec)

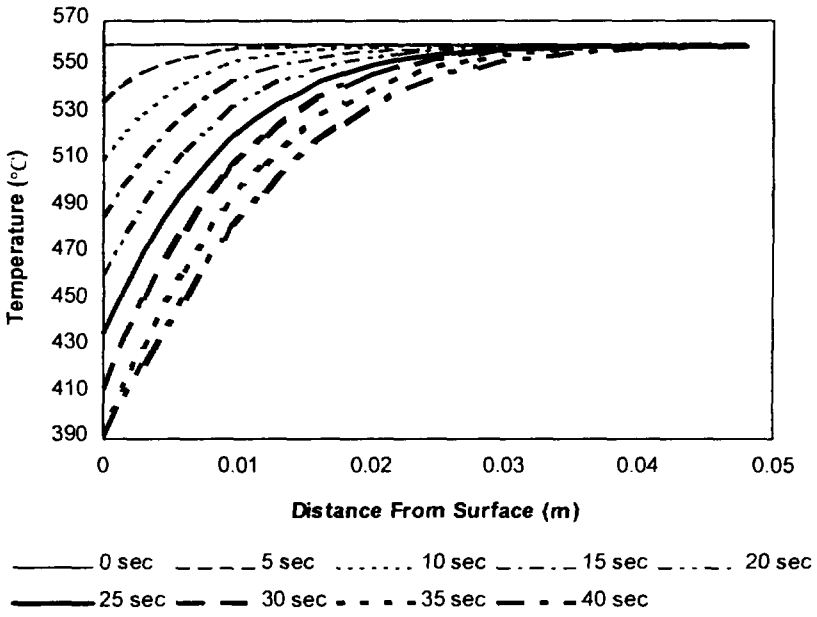

Figure 20 Temperature Distribution vs Distance From Surface(SS316 Plate)
(Film Coeff. f = 284000 J/sec-m^2-°C)

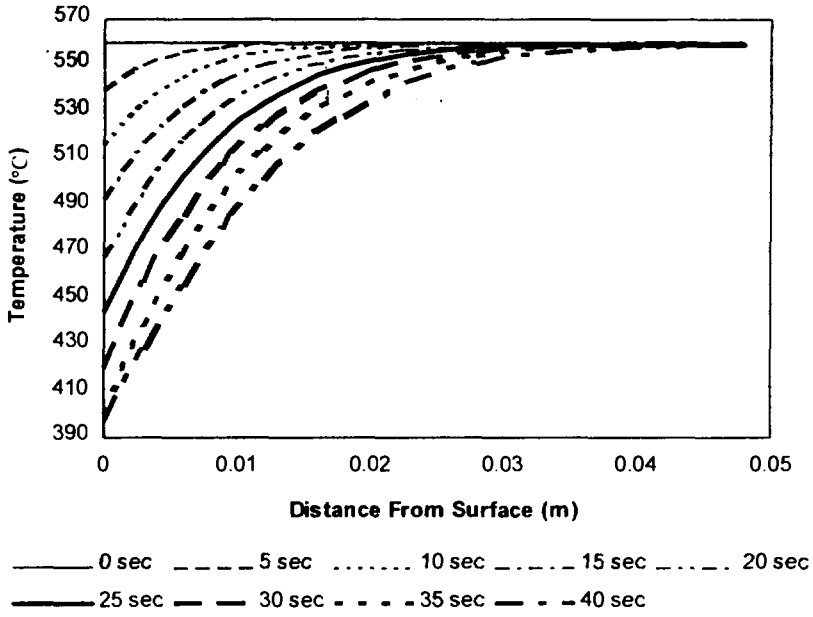

Figure 21 Temperature Distribution vs Distance From Surface(SS316 Plate)
(Film Coeff. f = 28400 J/sec-m^2-°C)

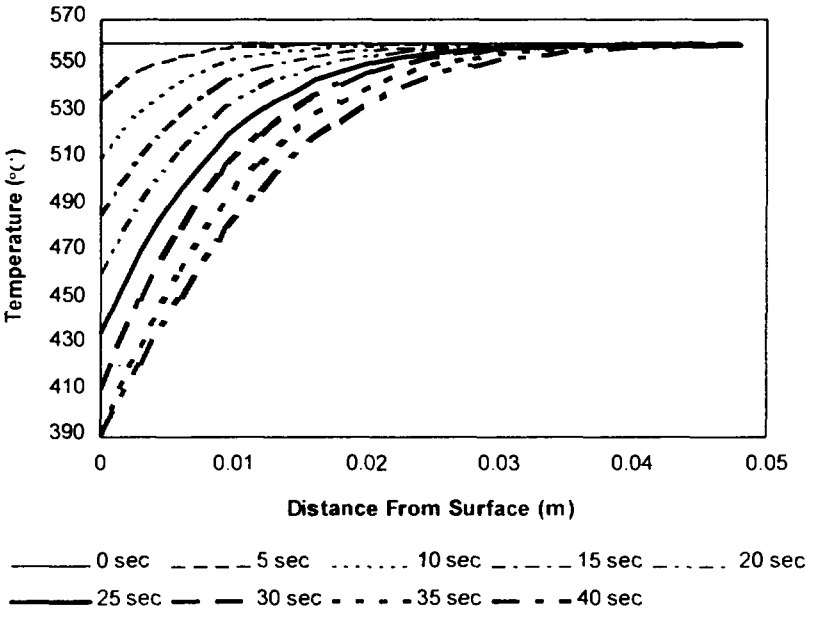

Figure 22 Temperature Distribution vs Distance From Surface(SS316 Plate)
(Film Coeff. f = 454400 J/sec-m^2-°C)

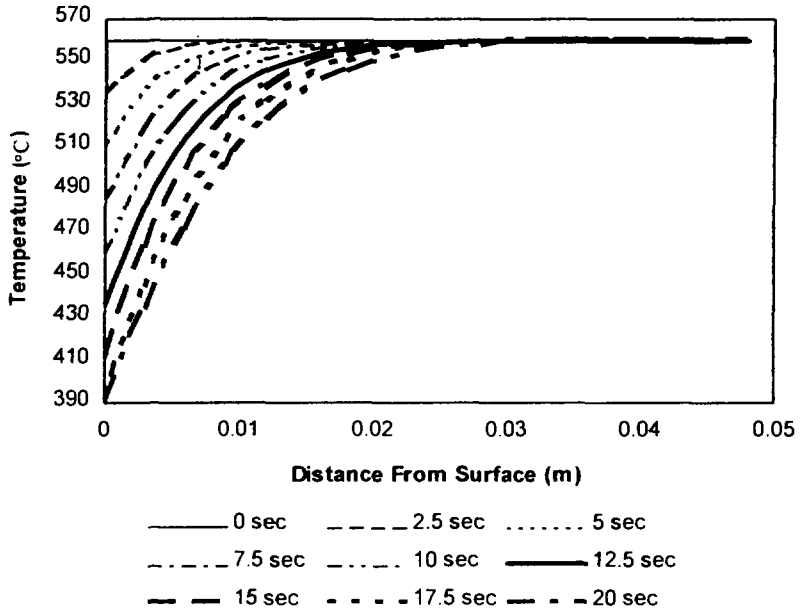

Figure 23 Temperature Distribution vs Distance From Surface(SS316 Plate)
(Film Coeff. f = 284000 J/sec-m^2-°C, Transient Rate 10 °C/sec)

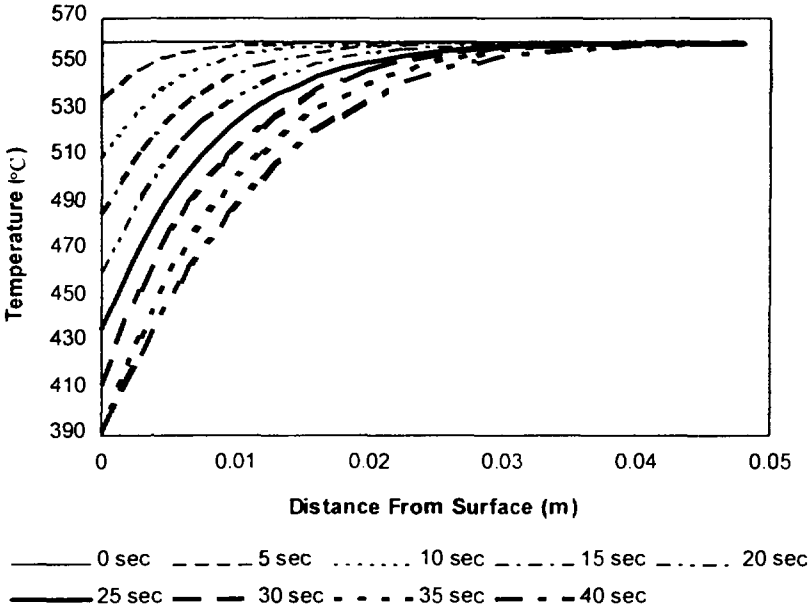

Figure 24 Temperature Distribution vs Distance From Surface
(I-718 and SS316 Plates, Film Coeff. f = 284000 J/sec-m^2-°C)

Performing Org. Report No.	Sponsoring Org. Report No.	Standard Report No.	INIS Subject Code
KAERI/TR-767/96			

Title / Subtitle

Preliminary Conceptual Design and Analysis on KALIMER Reactor Structures

Main Author and Dept.	Jong-Bum Kim / Development of LMR Design Technology
Researcher and Dept.	

Pub. Place	Taejon, Korea	**Pub. Org.**	KAERI	**Pub. Date**	Oct., 1996
Page	60 P	**Fig. and Tab.**	Yes(o), No( )	**Size**	26 cm
Note					
Classified	Open(o), Outside( ), __Class		**Report Type**		
Sponsoring Org.			**Contract No.**		

Abstract (About 300 Words)

The objectives of this study are to perform preliminary conceptual design and structural analyses for KALIMER(Korea Advanced Liquid Metal Reactor) reactor structures to assess the design feasibility and to identify detailed analysis requirements. The principal reactor structures are the reactor vessel, containment vessel and closure head which form the primary pressure boundary, support barrel and core support structure which provide core support and core restraint, the reactor vessel liner, separation plate and thermal baffle which, in conjunction with the support barrel separate the hot and cold pools, and the upper internal structures which support the core control system structures. Demonstration of design feasibility for the reactor structures requires system thermal-hydraulic, structural, and neutronic analyses. Component responses to these system loads would be compared with design limits to assess the design adequacy. However, KALIMER thermal hydraulic system analysis results and neutronic analysis results are not available at present, only limited preliminary structural analyses have been performed with the assumptions on the thermal loads. The responses of reactor vessel and reactor internal structures were based on the temperature difference of core inlet and outlet and on engineering judgments. Thermal stresses from the assumed temperatures were calculated using ANSYS code through parametric finite element heat transfer and elastic stress analyses. While, based on the results of preliminary conceptual design and structural analyses, the ASME Code limits for the reactor structures were satisfied for the pressure boundary, the needs for inelastic analyses were indicated for evaluation of design adequacy of the support barrel and the thermal liner. To reduce thermal striping effects in the bottom area of UIS due to up-flowing sodium from reactor core, installation of Inconel-718 liner to the bottom area was proposed, and to mitigate thermal shock loads, additional stainless steel liner was also suggested. The design feasibilities of these were validated through simplified preliminary analyses. In conceptual design phase, the implementation of these results will be made for the design of the reactor structures and the reactor internal structures in conjunction with the thermal hydraulic, neutronic, and seismic analyses results.

Subject Keywords (About 10 Words)

KALIMER, Reactor Structures, High Temperature, Thermal Stress, Thermal Striping, Thermal Shock

서 지 정 보 양 식			
수행기관 보고서번호	위탁기관 보고서번호	표준보고서번호	INIS 주제코드
KAERI/TR-767/96			
제목 /부제	칼리머 원자로구조에 대한 예비 개념설계 및 해석		
주저자 및 부서명	김 종 범 / 액체금속로 설계기술개발		
공동연구자 및 부서명			

발 행 지	한국, 대전	발행기관	한국원자력(연)	발행일	1996.10.
페 이 지	60 P	도 표	유(o), 무( )	크 기	26 cm
참고사항					
비밀여부	공개 (o), 대외비( ), __급비밀	보 고 서 종 류			
연구위탁기관		계 약 번 호			

초록 (300 단어 내외)

본 연구의 목적은 칼리머(KALIMER, Korea Advanced Liquid MEtal Reactor) 원자로 구조물에 대한 예비 개념설계와 예비해석을 수행하여 현재의 예비 개념 연구단계에서의 설계타당성을 분석하고 예측 가능한 문제점을 도출하는 데 있다. 칼리머 원자로 구조물은 원자로용기, 격납용기, 및 원자로 뚜껑으로써 일차 압력경계를 이루고 있으며, 원자로 내부 구조물은 노심의 지지와 구속을 해주는 노심 지지구조물과 노심 제어계통을 지지해주는 노내 상부구조물, 및 고온과 저온의 소디움 풀을 격리하는 역할을 해주고 있는 원자로용기 라이너, 격리판, 열 배플, 및 지지배럴로 구성되어 있다. 원자로구조물의 구조건전성을 보이기 위해서는 계통 열유동해석이 선행되어야 하지만 현재 칼리머에 대한 계통해석 자료가 없기 때문에 본 연구에서는 주요 부품의 열 하중에 대한 제한적인 예비해석을 수행하였다. 해석에 사용된 열 하중은 노심을 통과하는 소디움의 온도 상승, 고온과 저온 소디움 풀의 온도차, 및 각각의 핵연료집합체를 통과하는 소디움의 온도차 등이다. 원자로 용기 및 원자로 내부구조물에 대한 열전달과 열응력 해석은 노심 입출구의 설계온도와 공학적 판단에 기초한 가정치를 사용하였으며 해석에는 상용 유한요소해석 코드인 ANSYS가 이용되었다. 해석 결과 원자로용기, 격납용기, 원자로 뚜껑, 열 배플, 및 격리판에 대해서는 ASME 코드의 설계제한치를 잘 만족하였고 원자로용기 라이너와 지지배럴에 대해서는 설계 타당성과 구조 건전성을 입증하기 위하여 향후 지지배럴의 내벽에 설치할 피막을 고려한 상세한 해석과 부분적인 비탄성해석의 필요성이 대두되었다. 그리고 노심으로부터 올라오는 소디움의 스트라이핑 영향을 줄이기 위하여 노내 상부구조물 하부판에 인코넬 718 라이너의 도입을 제안하였고 또한 열충격 하중을 완화하기 위하여 추가적으로 스테인레스강으로 만든 라이너의 도입을 제안하였으며 단순 예비해석을 통하여 이에 대한 타당성을 입증하였다. 향후 좀 더 자세한 설계자료와 스트라이핑 하중을 보다 정확하게 산출해 낼 수 있는 실험자료 및 열유동 해석자료를 사용한 상세해석이 요구된다.

주제명 키워드 (10 단어 내외)

KALIMER, 원자로구조, 고온구조, 열응력, 열 스트라이핑, 열충격